ERDC/CERL TR-22-11

Construction Engineering
Research Laboratory

US Army Corps
of Engineers®
Engineer Research and
Development Center

ERDC
ENGINEER RESEARCH & DEVELOPMENT CENTER

White Sands Missile Range Thurgood Canyon Watershed

Analysis of Range Road 7 for Development of Best Management Practices and Recommendations

Daniel R. Gambill, Matthew M. Stoklosa, Sean A. Matus,
Heidi R. Howard, and Garrett R. Feezor

September 2022

The US Army Engineer Research and Development Center (ERDC) solves the nation's toughest engineering and environmental challenges. ERDC develops innovative solutions in civil and military engineering, geospatial sciences, water resources, and environmental sciences for the Army, the Department of Defense, civilian agencies, and our nation's public good. Find out more at www.erdc.usace.army.mil.

To search for other technical reports published by ERDC, visit the ERDC online library at https://erdclibrary.on.worldcat.org/discovery.

ERDC/CERL TR-22-11
September 2022

White Sands Missile Range Thurgood Canyon Watershed

Analysis of Range Road 7 for Development of Best Management Practices and Recommendations

Daniel R. Gambill, Matthew M. Stoklosa, Sean A. Matus, Heidi R. Howard, and Garrett R. Feezor

US Army Engineer Research and Development Center (ERDC)
Construction Engineering Research Laboratory (CERL)
2902 Newmark Dr.
Champaign, IL 61822

Final Report

Prepared for White Sands Missile Range, Integrated Training Area Management, WSMR, NM 88002.

Under MIPR 11305306

Abstract

Thurgood Canyon, located on White Sands Missile Range (WSMR), contains an alluvial fan that is bisected by a primary installation road and is in the proximity of sensitive fish habitats. This project was initiated to determine if and how sensitive fish habitats at the base of the fan are impacted by the existing drainage infrastructure and to assess the condition and sustainability of the existing transportation infrastructure. Findings show that the current drainage infrastructure maintains flow energy and sediment carrying capacity further down the fan than would occur in its absence. However, frequent to moderately rare (small to medium) flood events dissipate over 2 km from sensitive habitat, and overland flow and sediment do not reach the base of the fan. Controlled flow diversion is recommended upstream of the road to mitigate infrastructure or habitat impacts during very rare (very large) flood events. A comprehensive operation and management approach is presented to achieve sustainable transportation infrastructure and reduce the likelihood of impacts to the sensitive habitat.

Contents

Figures and Tables

Figures

Tables

Preface

This study was conducted for White Sands Missile Range under MIPR 11305306, "Analysis of Range Road 7 for Development of Best Management Practices." The technical monitor was Mr. James J. Thompson, Test Resources Support Office, Materiel Test Directorate, White Sands Missile Range, NM, 88002.

The work was performed by the Training Lands & Heritage Branch of the Operational Science & Engineering Division, US Army Engineer Research and Development Center, Construction Engineering Research Laboratory (ERDC-CERL). At the time of publication, Dr. Chris Rewerts was chief; Dr. George Calfas was division chief; and James P. Allen, was the technical director for Operational Science and Engineering. The deputy director of ERDC-CERL was Ms. Michelle Hanson, and the director was Dr. Andrew J. Nelson.

COL Christian Patterson was commander of ERDC, and Dr. David W. Pittman was the director.

1 Introduction

1.1 Background

The warfighter requires realistic training conditions to develop the most capable soldiers, which requires that Army training lands and ranges must simulate a realistic environment. Access to training lands is also paramount to maintain readiness. Given the diverse environments and terrain of military installations, access to realistic training lands might require infrastructure and training ranges be built within riverine systems and on unstable geologic formations.

At White Sands Missile Range (WSMR), built infrastructure is located within and across active fluvial channels, which require either channelization or rerouting of the flow. The presence of transportation infrastructure can potentially alter the natural flow and sediment loads, creating conditions that might degrade the natural environment. Arid alluvial fans are episodic, changing little during dry or even average years, but producing tremendous geomorphological changes during large runoff events or wet years (MacArthur et al. 1990). AR 200-1 requires the Army to be good stewards of their land, which might require development and deployment of best management practices (BMP) to lessen potential environmental degradation while promoting access to training and testing lands (DA 2007).

Alluvial fans in arid environments are formed when sediment laden runoff from steep mountain sides drains onto a low-lying plain. As the channel slope becomes flatter on the adjacent plain, the flow loses a significant amount of energy, depositing the sediments that build up the fan (Blair and McPherson 1994). The overland flow that runs off the mountains are forced by orographic precipitation during the wet season, leading to extended dry periods punctuated by large discharges (Richards and Moore 2003). The Thurgood Canyon valley contains sediment that ranges in size from silts to boulders, enabling large flow events to transport and deposit sediment onto the fan (Gomez-Viller and Garcia-Ruiz 2000).

The intense flow events within arid environments and resulting large sediment loads create scour and deposition that might negatively impact built

infrastructure, especially those present on alluvial fans. Transportation infrastructure built on alluvial fans in arid regions are particularly at risk due to the steep slope of the fan, increased velocity and debris load of the flows, the unpredictable braided nature of the channels, and the unconsolidated (easily erodible) fan sediments. Access to training lands can be limited during and following flow events due to flooded roadways, washouts, debris fields, or structure damage. These intense, short-lived flood events threaten the health and safety of Army personnel due to hazardous conditions, endangering the overall training mission. Beyond training mission impacts, altered hydrology due to range infrastructure can potentially jeopardize sensitive ecosystems located on or near the base of an alluvial fan and result in degraded water quality. Impacts to the natural system and endangered species can further affect the Army's training mission.

The only existing population of White Sands pupfish (*Cyprinodon tularosa*) lives within the White Sands Missile Range and the Holloman Air Force Base in southern New Mexico, primarily in springs and a stream located at the base of Thurgood Canyon's alluvial fan (Carman 2006). The pupfish was listed as a threatened species by the New Mexico State Game Commission in 1975. Although relatively plentiful where they occur, the pupfish are considered at risk because of their extremely limited distribution. Maintaining White Sands pupfish habitat, primarily the water sources that sustain them, is essential for their continued survival (Carman 2006). Primary threats include habitat alteration through construction or military training activities. The pupfish is protected by the Cooperative Agreement and Conservation Plan of 1994, which stipulates that the current population of the pupfish should be protected and measures be taken to increase their population.

1.2 Objectives

The objectives of this project are to (1) determine if and how the sensitive habitat of the pupfish, located at the base of the Thurgood Canyon's alluvial fan, is impacted by the existing drainage infrastructure, (2) assess the condition and sustainability of the existing transportation infrastructure, and (3) develop a comprehensive operation and management approach to achieve sustainable transportation infrastructure on the Thurgood Canyon alluvial fan and mitigate any impacts to the sensitive habitat located at the base of the fan.

1.3 Approach

The following methods were used to assess the environmental and infrastructure sustainability of the Thurgood Canyon alluvial fan: (1) estimation of the sediment load and flow characteristics under past and current conditions using field measurements and geographic information system (GIS) data, as well as hydrologic and hydraulic models, (2) determination of the preferred flow path of water runoff from the fan, (3) the development of operations and maintenance (O&M) approaches and BPMs, and (4) estimation of the new sedimentation and flow characteristics due to the proposed O&M recommendations. O&M approaches are designed to reduce ongoing maintenance of existing transportation infrastructure, reducing the frequency of washouts and mitigating environmental impacts downstream (DS). The findings herein are specific for the Thurgood Canyon alluvial fan, but the analysis and many of the BMP recommendations are universal for arid alluvial fans.

1.4 Location and project area

WSMR is located partially within the Tularosa Basin of the Chihuahuan Desert, including the San Andres and Oscura Mountains that bound the basin to the west (Figure 1). The region is arid and receives most of its annual precipitation from orographic precipitation during the North American Monsoon. As a result, numerous active alluvial fans are located within WSMR along the San Andres and Oscura Mountains.

The Thurgood Canyon basin covers 90.4 sq km (34.9 sq mi),* drains to the east, and is located directly west of the Carrizozo volcanic field (Figure 1). The canyon mouth (and alluvial fan apex) rests between Sheep Mountain and Capital Peak. Thurgood Canyon basin receives 350.5 mm (13.8 in.) of precipitation a year (Waltemeyer 2001). Basin soils are characterized by Bissett-Rock and Deama-Rock outcrop complexes in the uplands and river wash near the canyon floor. The soils are primarily gravelly clay loam and sandy loam, which are well drained to excessively drained with a very low water table and a very high infiltration rate. Infiltration rates range from 10 to 63.5 mm/hr (0.4 to 2.5 in./hr) and the depth of the water table is

* For a full list of the spelled-out forms of the units of measure used in this document and their conversions, please refer to *US Government Publishing Office Style Manual*, 31st ed. (Washington, DC: US Government Publishing Office, 2016), 245–252, https://www.govinfo.gov/content/pkg/GPO-STYLEMANUAL-2016/pdf/GPO-STYLEMANUAL-2016.pdf.

over 200 cm. Nonetheless, significant runoff is possible due to the very steep upland slopes and the steep slope of the main drainage channel.

Figure 1. Overview of WSMR, Tularosa Basin, and White Sands National Park (WSNP) (NPS 2022. Public Domain).

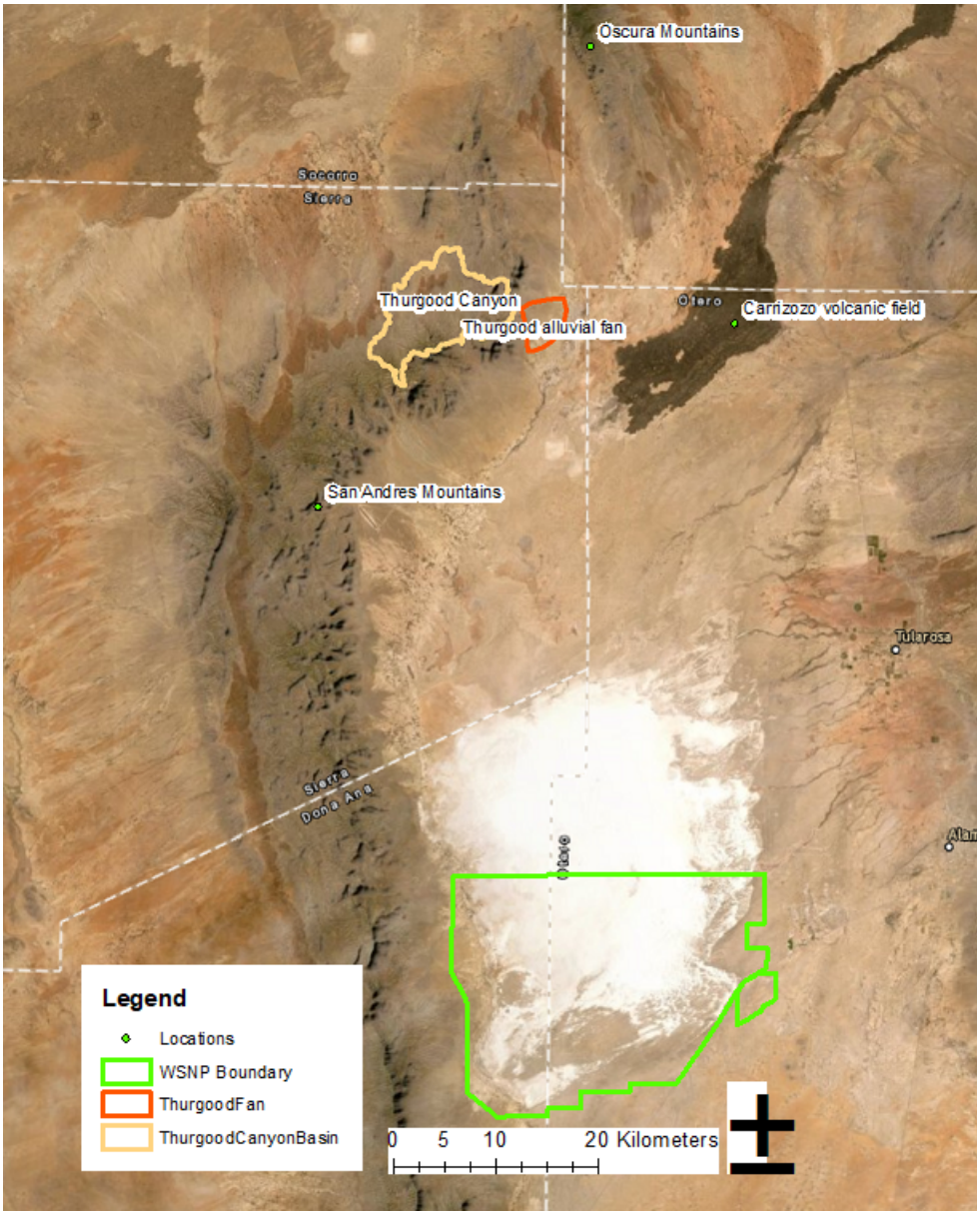

The Thurgood alluvial fan, located at the base of Thurgood Canyon, extends to the east and south, reaching almost to Salt Creek (Figure 2). The average slope of the fan is 0.017 m/m. The fan apex (top) rests at 1,360 m, and the bottom at 1,275 m. The fan length is approximately 4,700 m to the east and 5,300 m to the south. The fan is mostly gravelly sand with a portion of silty loam at the southern section. The primary US Department of

Agriculture (USDA) soil types on the fan are the Queencreek, Mimvres, and Chilicotal complexes (USACE 2018). Parent material ranging in size from gravel to boulders is also found along the main channel. The area is well drained to excessively drained with a very low water table.

Salt Creek is east of Thurgood fan and drains to the south within a closed basin. The upstream portion, known as Salt Springs, is located 1,000 meters east of the alluvial fan foot. Salt Creek runs into Big Salt Lake, where it becomes a salt flat during dry periods.

Figure 2. Thurgood Canyon basin boundary, alluvial fan, and surrounding area.

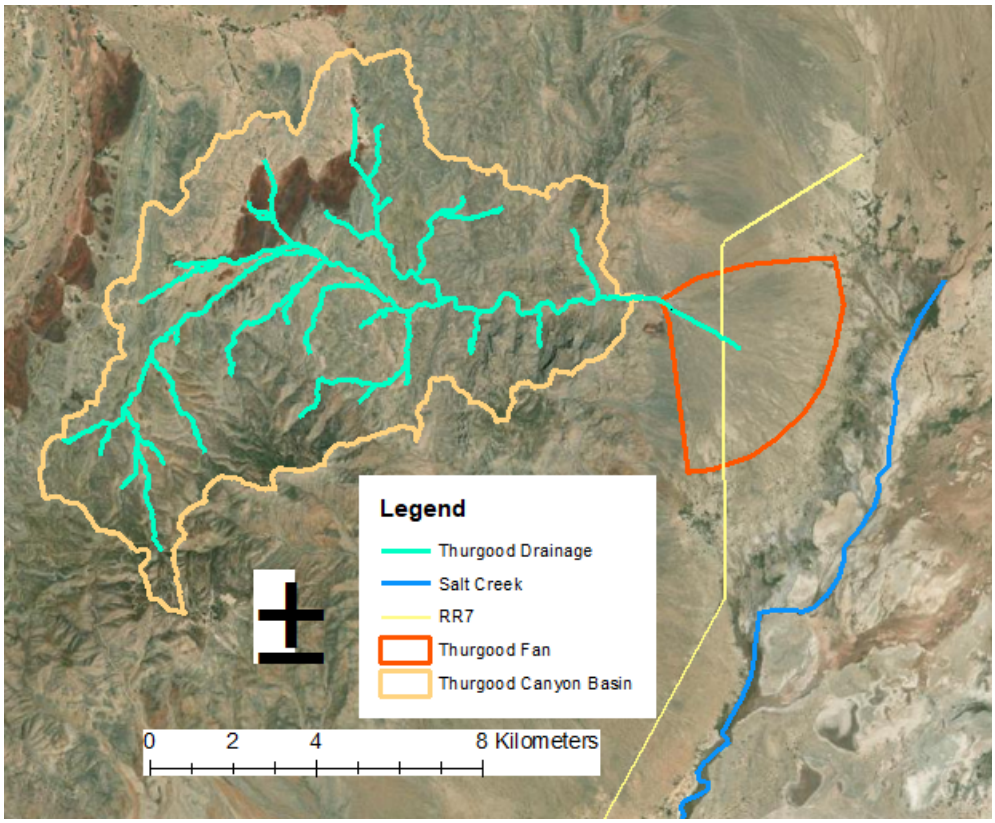

The Thurgood fan is traversed by RR7 1,650 m downstream of the fan apex along the main drainage channel. RR7 is the primary north–south range road within WSMR on the east side of the San Andres (Figure 3). The road is impacted annually by seasonal flood events. Debris in the road presents a driving hazard, and closures can limit access to major portions of the range.

Several berms direct the main channel flow through the primary (#1) culvert structure under RR7. The primary berm is located on the south side of

the main channel, beginning south of the fan apex and extending to RR7. Several other southerly berms direct surface runoff from the southern portion of the fan to smaller, secondary culverts under RR7 (culverts #2–5). Old channels south of the main channel (Figure 3) drain to the south and southeast and through these culverts. It is unknown if these culverts were designed and sized to provide local drainage for the southern portions of the alluvial fan or if they were sized to provide secondary drainage for flow coming from Thurgood Canyon.

Figure 3. Thurgood Canyon alluvial fan detailing locations of RR7, flow diversion berms, and exiting drainage infrastructure.

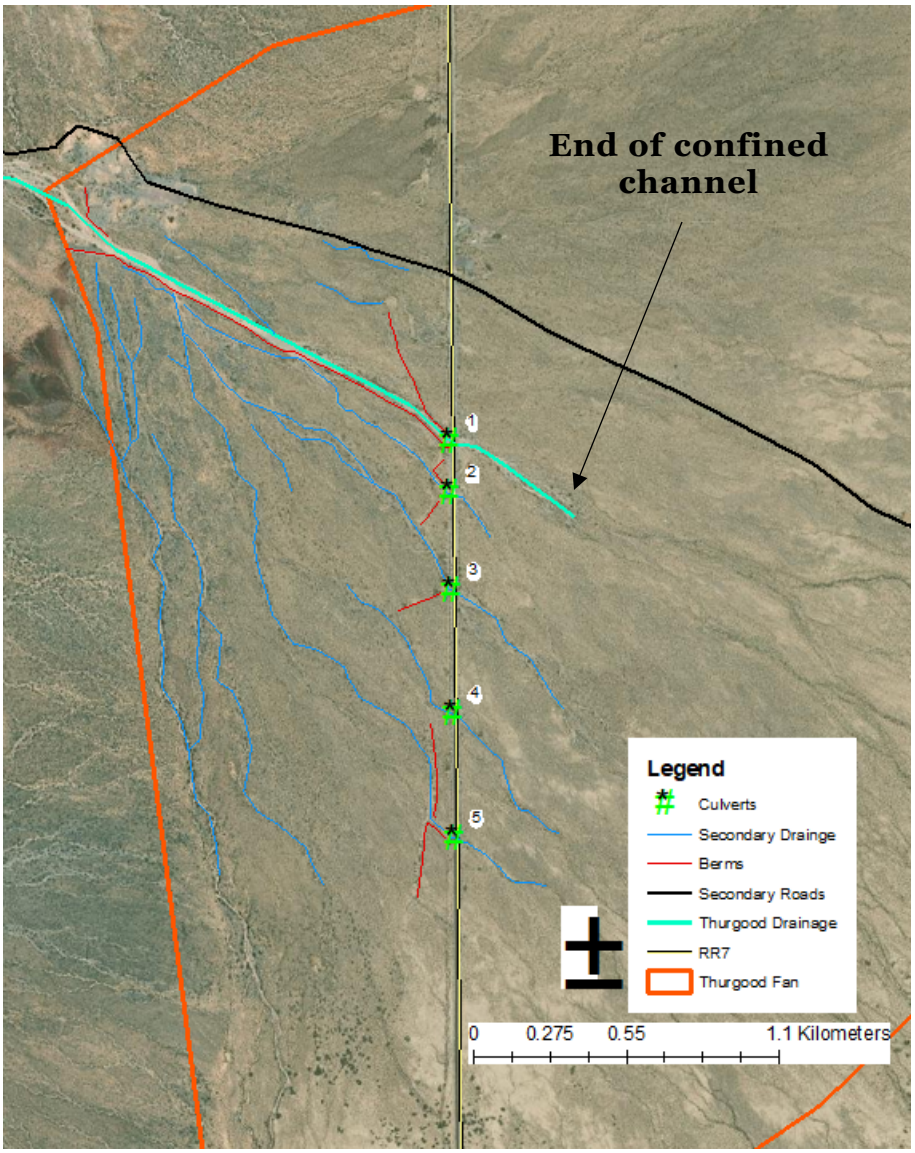

Culvert 1 is comprised of ten 2.44 × 2.44 m (8 × 8 ft) box culverts and is protected from scour on its abutments with gabion basket retaining walls.

In addition, the culvert is protected on the downstream side by a gabion mattress across the width of the culvert and extending 6 m downstream (Figure 4). Significant scour occurs at the downstream edge of the gabion mattress. The primary berm is made of dumped local material for most of its length but consists of riprap reinforced with wire mesh from RR7 to about 185 m upstream. To date, scour has not occurred along the reinforced section of the berm.

Figure 4. Culvert 1 upstream and downstream faces (*top left* and *top right*, respectively). Reinforced section of main berm (*middle left*) and gabion baskets (*middle right*). Gabion mattress scour BMP and toe scour (*bottom*).

Culverts 2–5, located south of the main channel, allow drainage under RR7 (Figure 5). All four culverts have a gabion basket drop structure just upstream. Culverts 2 and 4 are twin, 1.22 m (4 ft) diameter corrugated metal pipe (CMP) culverts with concrete headwalls. Culvert 4 is half plugged with sediment. Culvert 3 is a single, 1.22 m CMP with a concrete headwall. Culvert 5, furthest south, is a twin, 2.44 × 2.44 m box culvert.

Figure 5. Culverts 2–5 (*top left, clockwise*). Typical gabion basket drop structure (*bottom*).

The flow downstream of RR7 becomes unrestricted (Figure 6). The primary avulsion zone (where the confined channel ends) is approximately 475–500 m downstream of RR7. The avulsion zone is where surface flow begins to shift to new channel(s). These channel(s) change over time or

from event to event, and the flow spreads out over a wider portion of the fan (Figure 6). The area downstream of the confined channel is also called the active lobe. The active lobe is where a large amount of deposition begins due to the energy lost by the flow as it spreads out over a wider area and into small channels. Further downstream, different portions of the runoff evaporate, infiltrate into the soil, or reach Salt Creek via surface or subsurface drainage. A major difference of the Thurgood fan from a typical active alluvial fan is that the flow diversion berms and the RR7 structure on the Thurgood fan constrain the main channel, causing the active lobe of the fan to be located east of RR7.

Figure 6. Avulsion zone downstream of RR7 looking upstream (*left*) and downstream (*right*).

2 Methods

2.1 Sediment load

Measuring, characterizing, and modeling the sediment load from Thurgood Canyon was attempted in order assess potential impacts to pupfish habitat at the base of Thurgood fan. Total sediment load is estimated as a total of bedload and suspended load. Estimates of total sediment load for several events are used to determine the average annual sediment load.

2.1.1 Bedload field measurements

Generally, bedload is measured using either an active or passive sampling approach. Flow events at the study site are infrequent and access to the site is severely restricted due to military testing, so all samplers had to be installed, left unattended for a long period of time, and then recovered following flow events. An active sampler, such as the Helley-Smith, rests on the streambed and catches sediment in a net and is usually deployed and monitored for less than one hour. For the Thurgood project site, ERDC researchers chose to use a pit trap sampler (Sterling and Church 2002). Sterling and Church (2002) used pit trap samplers in large discharge, arid, and remote environments. They found that the Helley-Smith sampler worked well for small particles, but for larger particles, the sampler could not get a representative sample. The remote location, limited access, projected bedload particle size and quantity, and uncertainty of rainfall events required the use of a passive pit trap approach, which functions without a researcher being present.

The pit traps used were based on Church et al. (1991) and McMahon (2013) with small modifications. The design of the pit trap is shown in Figure 7. A corrugated five-foot section of HDPE pipe housed a five-gallon bucket. Tarp straps were secured to the outside of the pipe, keeping the bucket secured on the inside. Chains were added to aid in bucket retrieval. The traps were then buried into the main channel flush with the surface. The pit trap design was intended to withstand both the harsh climate and long-term deployment on the order of several months while also being of significant size and volume to ensure representative capture of the bedload.

Figure 7. Pit trap samplers and installation.

Four pit traps were installed into the bed of the main drainage channel between the fan apex and RR7. Two were installed near each ISCO-suspended sediment sampling site. Figure 8 shows the locations at which all gauges and samplers were installed. ISCO samplers and HOBO water level samples were also installed at these locations, allowing for the collection of suspended sediment samples and to record flow depth, respectively.

Figure 8. Pit trap and ISCO sampler and HOBO locations. Upstream (*lower left*) and downstream (*lower right*) gage and sampler locations shown in detail.

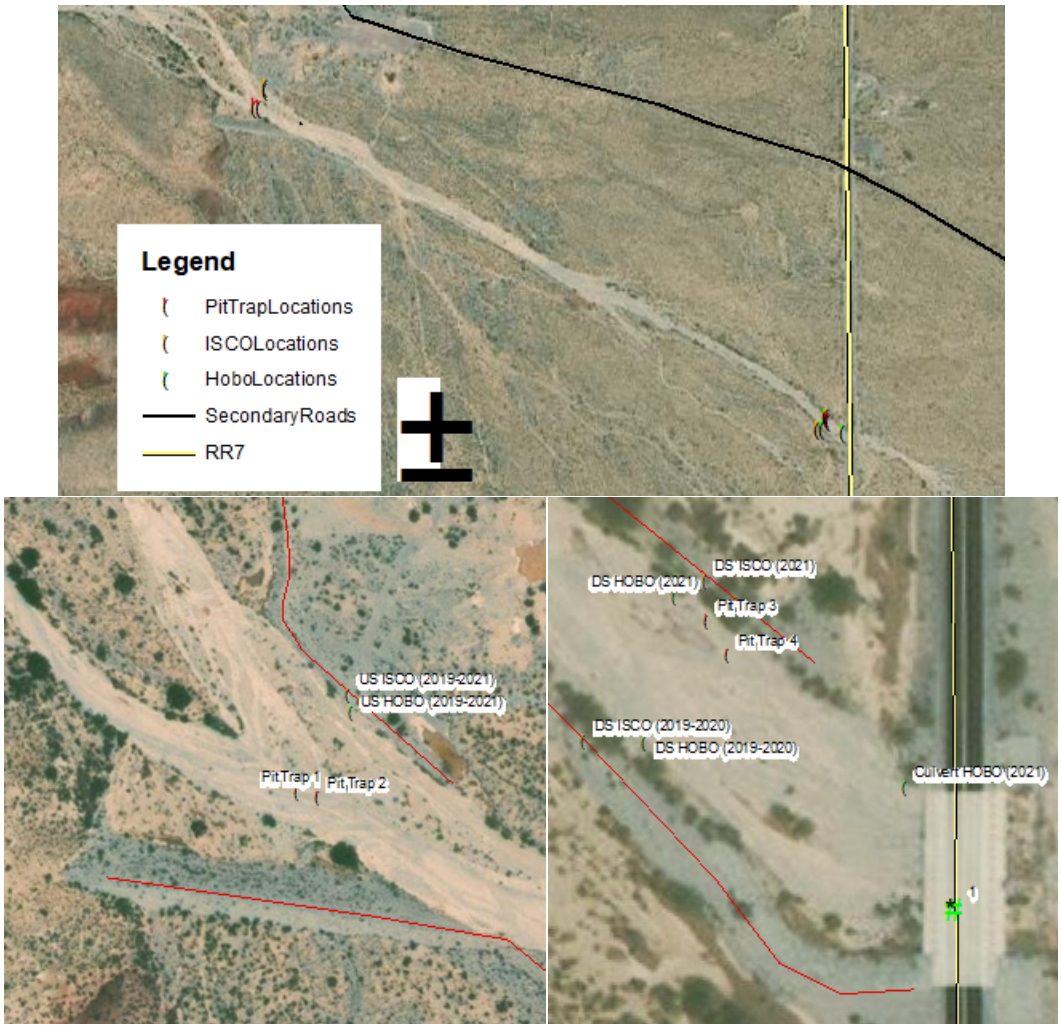

2.1.2 Downstream bed surface deposition

Downstream of the RR7 culvert, the main channel opens to allow unrestricted flow. After reaching a point of unrestricted flow, the runoff spreads out across the fan, distributing the energy of the flow over a greater area. The decrease in flow energy per unit area allows particles to fall out of suspension or stop moving as bedload. Large particles come to rest first as the flow energy decreases.

Large material often moves through the RR7 culverts before dropping out of the flow. This material can range from small cobble to large boulders. The material deposited can also create a gradient and a layer of larger particles on the channel bed called the amour layer. Material from select locations were categorized by size (sample boxes A–N). The area selected for

measurement was a square meter area; particles on the surface larger than gravel size were measured by hand on all three axes. Composite samples of the streambed were collected at the locations downstream of RR7 for sieve analysis. Sample locations are shown in Figure 9, while typical sample sites are shown in Figure 10. The locations were 250 and 130 m upstream of RR7 and 85, 200, 330, 475, and 600 m downstream of RR7. Sample boxes C and D (475 m downstream of RR7) were located approximately where the main channel becomes unrestricted.

Figure 9. Channel composite and surface sample locations (referenced distance upstream and downstream of RR7 structure).

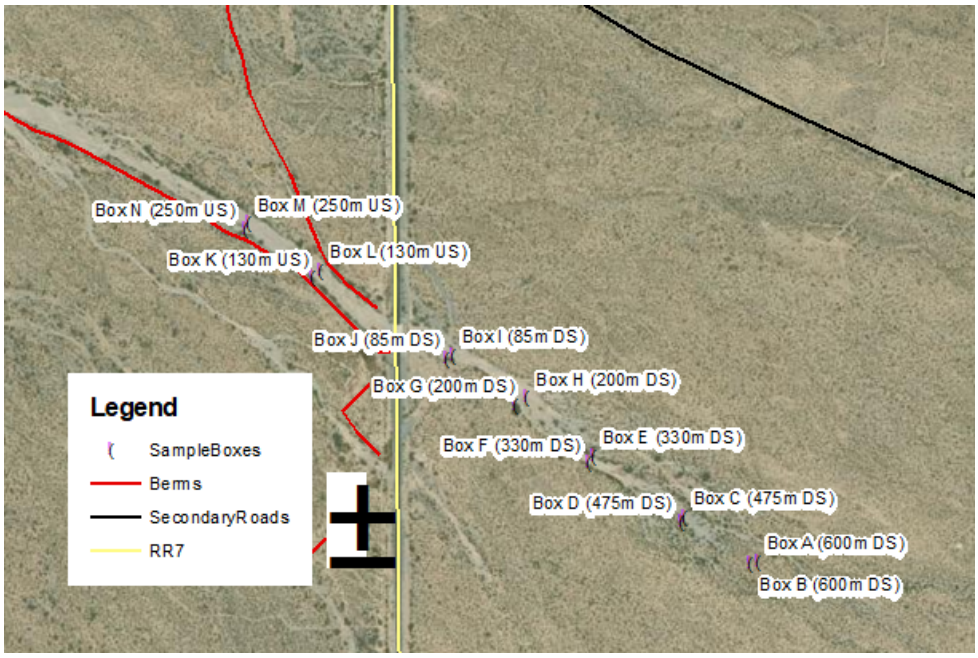

Figure 10. Typical composite and channel surface sample locations.

2.1.3 Bedload rate modeling

In addition to direct bedload field measurements, bedload was computed using the USDA Bedload Assessment in Gravel-bed Streams (BAGS) program (Pitlick et al. 2009). The BAGS software calculates bed load transport capacities on the basis of commonly available field data (surveyed cross sections and measured grain-size distributions) (Pitlick et al. 2009). BAGS implements up to six well-known bed load transport equations developed for gravel-bed rivers. Two of these equations require calibration, while three others were developed for particles only larger than sand (Wilcock 2009). Given the mixed sand and gravel sediments of Thurgood Canyon, the Wilcock and Crowe (2003) equation was implemented for the study basin.

2.1.4 Suspended sediment

Teledyne ISCO 3700C portable samplers were installed. The samplers are used to determine suspended sediment load during flow events (Figure 11). A configuration of 24 bottles, each 500 ml, was used to collect multiple, separate samples during flow events at 10-minute intervals, providing a sampling window of 240 minutes (4 hours). A water sensor was installed in the channel to activate the sampling program once water flow was detected. Samples were collected every ten minutes, allowing for a maximum four-hour sampling duration. One sampler was placed near the fan apex, while the other was placed just upstream of the RR7 culvert (Figure 8). The downstream sampler was located on the south side of the channel during the 2019 and 2020 sampling seasons. For the 2021 sampling season, the downstream sampler was moved to the north side of the channel due to a shift in the preferred flow path from the south to north side of the main channel. The ISCO samplers were placed in vented, white metal boxes, whereas the suction lines and intakes were placed in flexible metal conduit and PVC, respectively, to provide all components with protection from the harsh environment and animals (Figure 11).

Figure 11. Typical ISCO installation (*top*), typical installation of samples, suction lines, and intakes (*bottom*).

2.2 Laboratory methods

Sediment and water samples from the study site underwent particle size analyses and suspended sediment analysis, respectively. These analyses were completed to facilitate the development of sediment load rate models.

ERDC-CERL conducted all analyses of sediment samples. During the initial May 2019 site visit, composite substrate samples and surface samples were taken at each pit trap location. During the May 2021 site visit, one composite surface sample was taken at each sample location downstream of RR7. Two rainfall events occurred during 2019, July 6 and September 5, and resulted in pit trap samples. Each bedload sample was treated as a composite sample, giving two tests per pit trap per sampling event.

Suspended sediment samples were collected by the upstream ISCO sampler during the July 2019 event, while the downstream sampler did not activate. Neither sampler activated during the September 2019 event. In 2021, samples were collected during several events. The downstream ISCO sampler collected samples on 27 June 2021 and 4 September 2021. The

upstream ISCO sampler collected samples on 6 July 2021. During each 2021 sampling event, only one ISCO sampled each time. Table 1 gives the information for samples taken at WSMR.

Table 1. Sample collection summary.

Time	Location	Description	Number of samples
25 May 2019	Pit traps 1–4	Native bed samples	14
6 July 2019	Pit traps 2–4	Bedload	6
6 July 2019	US ISCO	Suspended sediments	6
15 Sept. 2019	Pit traps 2–4	Bedload	6
29 May 2021	Boxes A–J	Surface samples and amour layer samples	5
27 June 2021	DS ISCO	Suspended sediments	16
6 July 2021	US ISCO	Suspended sediments	6
4 Sept. 2021	DS ISCO	Suspended sediments	24

Particle size analyses and suspended sediment analyses were completed for all samples as required. Detailed information about lab methods can be found in Appendix A.

2.3 GIS and lidar assessments

Lidar and aerial imagery were used to assess scour, erosion, and deposition along the main drainage channel, south of the main channel, and downstream of RR7 over time. In particular, scour along the main channel berm was analyzed, and locations of weir flow from the main channel as well as subsequent drainage channels were determined. Downstream of RR7, areas of deposition, areas of erosion, and preferential flow paths were determined. In addition, the research team looked for evidence of overland flow reaching Salt Creek from Thurgood Canyon.

Aerial images of the study site were reviewed, including images from October 1996, July 2005, January 2007, August 2009, October 2013, November 2017, and August 2019.

The WSMR Integrated Training Area Management Program (ITAM) office provided lidar collected in 2013. An additional lidar data set was obtained from the USGS 3D Elevation Program (3DEP) flown between late 2018 and early 2019. Site-specific lidar was also collected using an unmanned aerial system (UAS) mounted with a Geodetics GEO-MMS package with a Velodyne VLP-16 lidar. The Thurgood alluvial fan was flown March 2021.

In addition, aerial images obtained by the USGS National Agricultural Imagery Program (NAIP) in 2011 and 2020 were used to assess changes to vegetation. Table 2 provides a summary of data sets.

Table 2. GIS data sets.

Data Set	Time	Coverage	Native Resolution
WSMR Lidar	2013	Full Fan	75 cm
USGS Lidar	2019	Full Fan	1 m
Local Lidar	2021	Study Area Channel	75 cm
NAIP Aerial Image	2011	Full Fan	60 cm
NAIP Aerial Image	2020	Full Fan	1 m

Digital elevation models (DEMs) created from the collected lidar were used to determine the shape and size of the primary berm scour holes over time and to assess the drainage patterns and subwatershed areas to the south of the main channel and west of RR7 (Figure 12). A slope, watershed, and preferential flow path assessment was completed using the 2019 topographic data set.

The erosion and deposition that occurred between each of the collection years was mapped using the DEMs. Using ESRI ArcPro, the DEMs were resampled to ensure that they were on identical grids. The rasters were subtracted to find the elevation difference, creating a DEM, where positive and negative values indicate deposition and erosion, respectively. This process was completed between each temporally adjacent data set to determine the terrain changes over multiple time steps. The differences between DEMs show where new channels have formed or existing channels have evolved due to erosion and deposition caused by intermittent flow events. Each difference raster contains negative values where erosion occurred in red and positive values where deposition occurred in blue. Darker shades indicate a larger magnitude of erosion or deposition measured in meters of change. Values close to zero are white and indicate no change to terrain.

Figure 12. 2013 (*top left*), 2019 (*top right*), and 2021 (*bottom*) DEMs created from lidar.

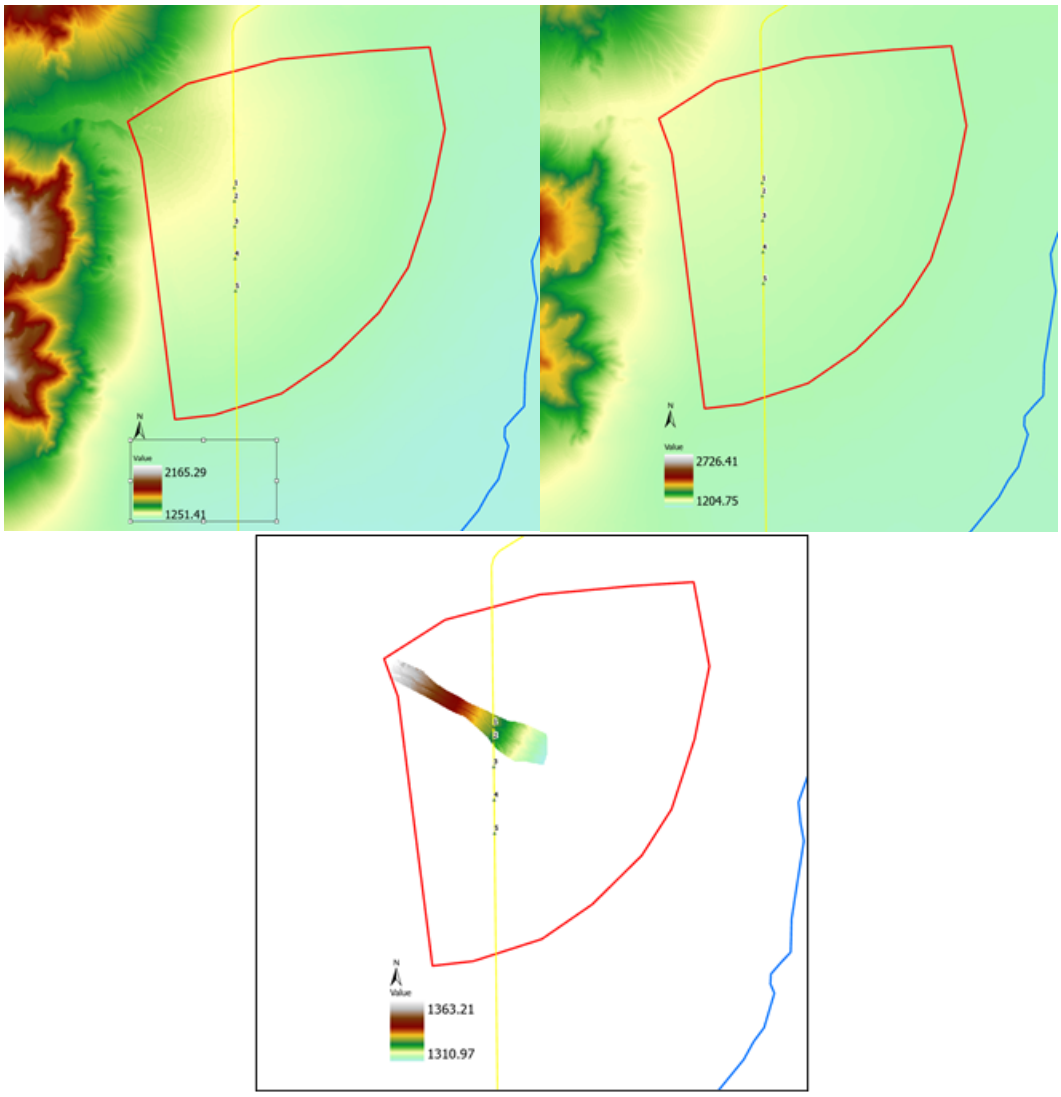

Changes in vegetation were analyzed using aerial images and used as a proxy to detect changes to the fan surface. Using the infrared (IR) band, the normalized difference vegetation index (*NDVI*) could be calculated for both years in ArcPro. NDVI is a dimensionless measure of the density of green in an image derived from the difference in near-infrared radiation (*NIR*) and visible red radiation (*R*) (Weier and Herring 2000).

$$NDVI = \frac{NIR - R}{NIR + R}$$

The values of NDVI range from -1 to 1, where values closest to 1 indicate the highest vegetation density, 0 indicates no vegetation, and values near -

1 indicate disturbances like clouds or water. ArcPro adjusts the NDVI formula to create a range from 0 to 200 to fit into an 8-bit color ramp.

$$NDVI = \frac{NIR - R}{NIR + R} \times 100 + 100$$

Using the NDVI rasters created in ArcPro for the 2011 and 2020 imagery, the change in vegetation in that timeframe was determined. A cell-by-cell difference was calculated, which yielded a raster that shows where vegetation density decreased, indicating a loss of vegetation due to erosion undermining that area. The difference raster also shows where the density of vegetation increased, indicating healthy vegetation growth due to an increase in available water. This approach is limited in that it does not indicate erosion if vegetation was already absent in an area.

2.4 Water level data loggers

HOBO Water Level Data Loggers were installed near the ISCO samplers and the RR7 culvert (Figure 8) to provide continuous monitoring of pressure and temperature at 10-minute intervals (Figure 13). The downstream HOBO was relocated with the downstream ISCO at the beginning of the 2021 sampling season, while the sensor directly upstream of RR7 was installed at the same time. HOBO 30-Foot Depth Water Level Data Loggers (Part # U20-001-01) were utilized and were factory calibrated and designed for continuous use. The sensors were housed in perforated PVC tubes to protect them from the harsh environment and large bedload particles (Figure 14). Survey data were used at sensor locations to develop rating curves, which can be used with the logged flow-depth data to generate flow hydrographs, using the same methods implemented at USGS gauge sites.

Figure 13. Raw HOBO atmospheric pressure and temperature output from 2021.

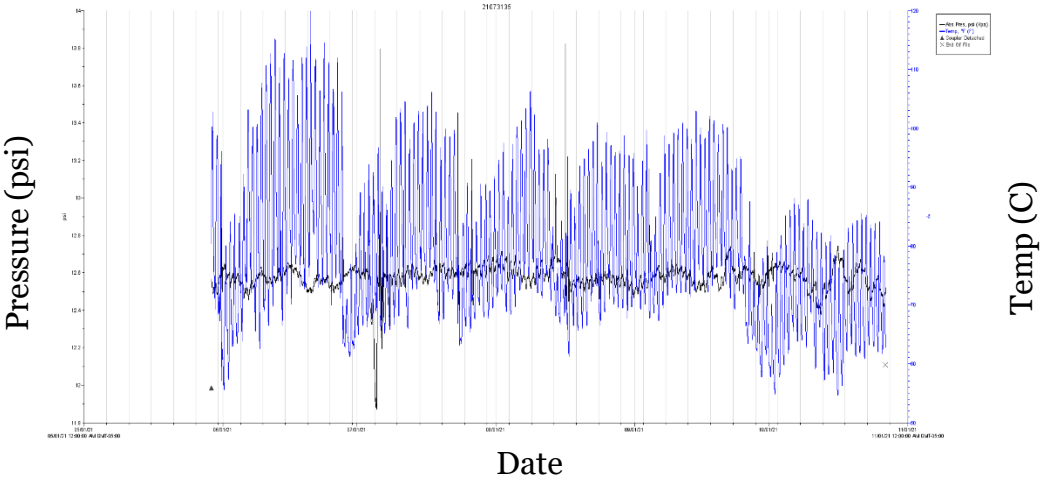

Figure 14. Typical HOBO installations.

2.5 Hydrology model

The Hydrologic Engineering Center Hydrologic Modeling System (HEC-HMS) accomplishes the physical representation of a watershed with a basin-scale model, which simulates hydrologic processes such as soil infiltration, overland flow, and hydrologic routing. Widely available GIS data (i.e., topographic, soils, land use, and drainage networks) are used to create a physically based representation of a basin. HEC-HMS accepts gridded, long-term precipitation data, which are transformed into excess saturation and infiltration runoff at the gridded subbasin scale using the gridded soil moisture accounting (SMA) method. The excess runoff is routed overland through the ModClark transform method and into channel reaches to the basin outlet using the Muskingum-Cunge method.

The catchment and stream network for the model was delineated from the 2019 DEM (Figure 15). The minimum contributing area to initiate a

stream was set to the default for each study subbasin (1% of the largest contributing area within each subbasin).

Figure 15. Thurgood watershed HEC-HMS model schematic.

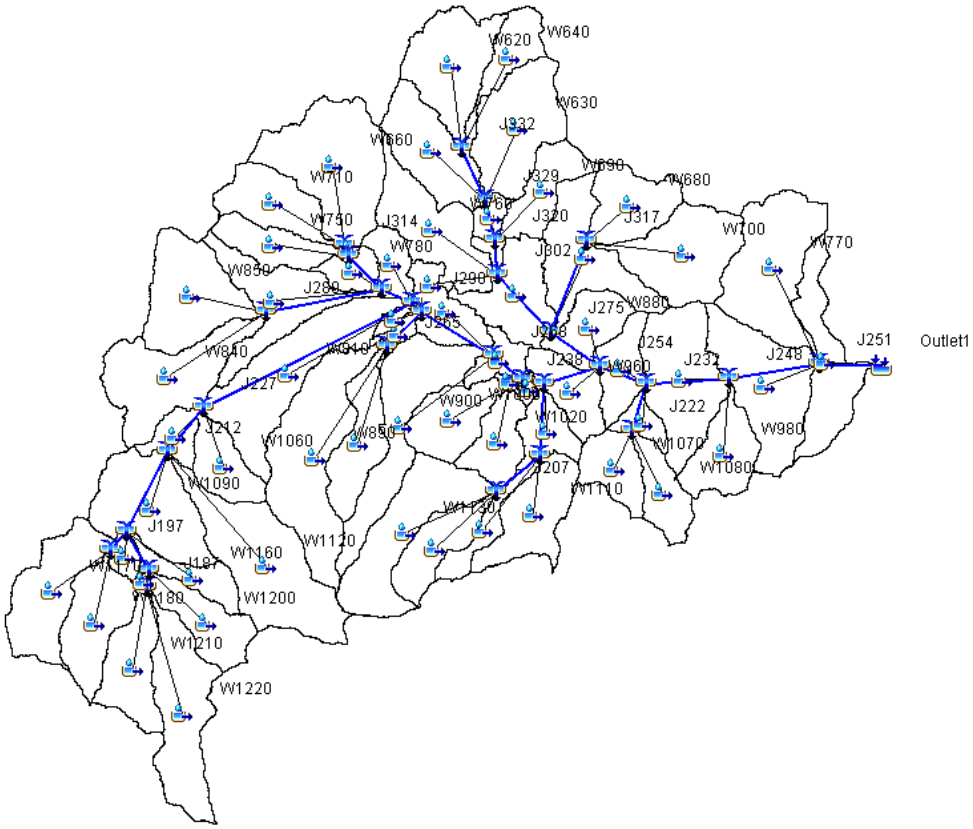

Detailed information about the HEC-HMS model setup, initial parameter values, and calibration methods can be found in Appendix B.

2.6 Hydraulics model

A steady, 1D Hydrologic Engineering Center River Analysis System (HEC-RAS) model was developed from the mouth of Thurgood Canyon to just below RR7 (Figure 16). The four culverts to the south of the main channel were also incorporated into the model. The hydraulic model was developed through field surveys with some additional definition of channel overbank areas, roadway crests, and berms using the DEM data. All additional required parameters were determined during surveying. A wide range of flow profiles were produced to develop rating curves (e.g., flow rate vs. flow depth, flow rate vs. flow velocity) at each HOBO gauge location. The

model terminated downstream of RR7 at the point that the main channel becomes unconfined.

Three versions of the HEC-RAS model were developed corresponding to the three available DEM data sets, and a fourth version to test proposed flow control BMPs.

Figure 16. Thurgood fan HEC-RAS model schematic.

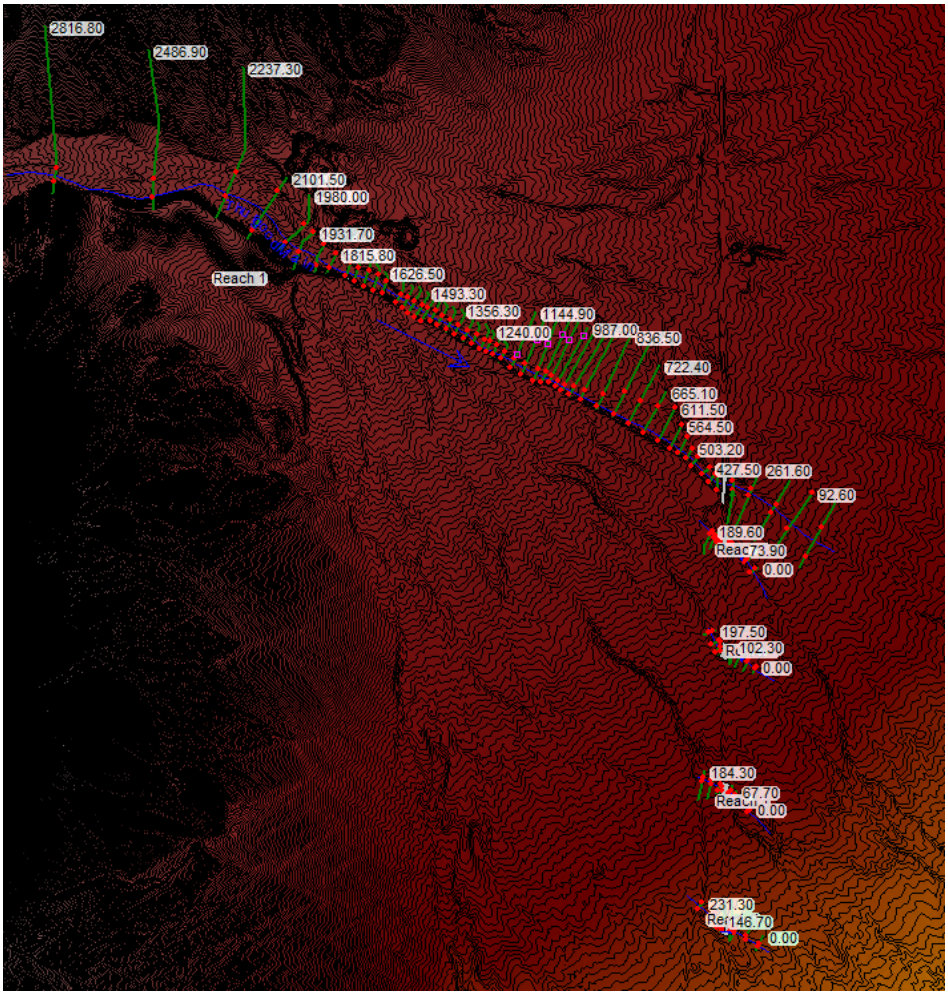

2.7 Previous work and findings

Table 3 shows estimated peak flows from Thurgood Canyon from a study by USACE Tulsa District (USACE 2018). Their estimates were compared with the streamflow regression equations for floods ranging from the 2-year to the 500-year (Waltemeyer 2008). Differences between smaller storm sizes where the calculated flows were higher than the USGS estimated flows occurred, but for larger storms, the values were similar.

Table 3. Thurgood Canyon Watershed storm calculated outflow comparison with USGS estimated outflows.

Storm Size	USGS Max Outflow (ft^3/s)	Calculated Max Outflow (ft^3/s)
2 yr	20.9	71.9
5 yr	41.5	92.4
10 yr	59.9	108.6
25 yr	88.9	131.2
50 yr	115.3	149.7
100 yr	145.9	169.5
500 yr	236.9	222.0

The discrepancy for the smaller storms could be due to the values chosen for the model parameters. Because of the inability to calibrate the watershed model to measured stream gauge values, losses were estimated to be zero throughout the basin. This assumption will lead to larger outflow volumes with smaller storm sizes, although for larger storms, losses will become negligible as their effect is diminished with increasing storm volume size.

A study by Naus et al. (2014) compiled hydrologic and water quality data for White Sands pupfish habitat and nonhabitat areas in the northern Tularosa Basin from 1911–2008. One study site, Site 4 at RR7, was located on Salt Creek at the base of the Thurgood alluvial fan. From 1995 to 2008, the USGS periodically collected water quality data, including field measurements and water samples for chemical analysis, in conjunction with instantaneous streamflow measurements. At the Salt Creek near Tularosa gaging station, suspended-sediment concentrations ranged from 4 to 1,570 mg/L from 1999 through 2008 over 57 separate samples. Over the same period, Site 4 was sampled three times and concentrations of 608, 1,210, and 3,430 mg/L were recorded. The latter record was the highest concentration recorded at any site. Perchlorate was detected at 16 µg/L in one sample collected in 2000 from the Salt Creek Site 4 at RR7; this was the only sample collected with a detectable perchlorate. The potential cause(s) of these anomalous results were not investigated.

3 Results and Discussion

3.1 Observed streamflow

The upstream and downstream HOBO units began recording on 1 June 2019 and continued through October 2021 with only limited interruptions. The third unit, located just upstream of RR7, recorded from the end of May through October 2021. Both deployed units missed the 25 May 2019 flow event because neither were programed to activate until the following week. The upstream unit was the most inconsistent with regards to capturing flow events due to its placement near the north side of the relatively wide main channel at that location. No flow events were recorded during 2020. The placement was selected to better protect the sensor from large particles moving downstream during the flow events.

The downstream unit (and the unit just upstream of RR7) were more consistent in capturing flow events due to the relatively narrow channel at this location. Nonetheless, no observed data were recorded at the downstream location during 2020 despite evidence that flow events occurred during that calendar year. During the May 2021 field visit, observations indicated that the primary drainage path near the downstream gauge site seemed to have shifted from the south side to the north side of the main drainage channel. As a result, the water sampler and HOBO unit were redeployed to the north side in May 2021.

Survey data were recorded at all deployed HOBO locations in May of 2019 and 2021 to develop the most accurate rating curves possible. The shape of the main drainage channel could change significantly from event to event due to the large amounts of material scoured or deposited at various locations. To account for these changes, different rating curves were developed for both 2019 and 2021. Observed flow hydrographs are shown in Figure 17.

Figure 17. Observed flow hydrographs for 2019 (*top*) and 2021 (*bottom*).

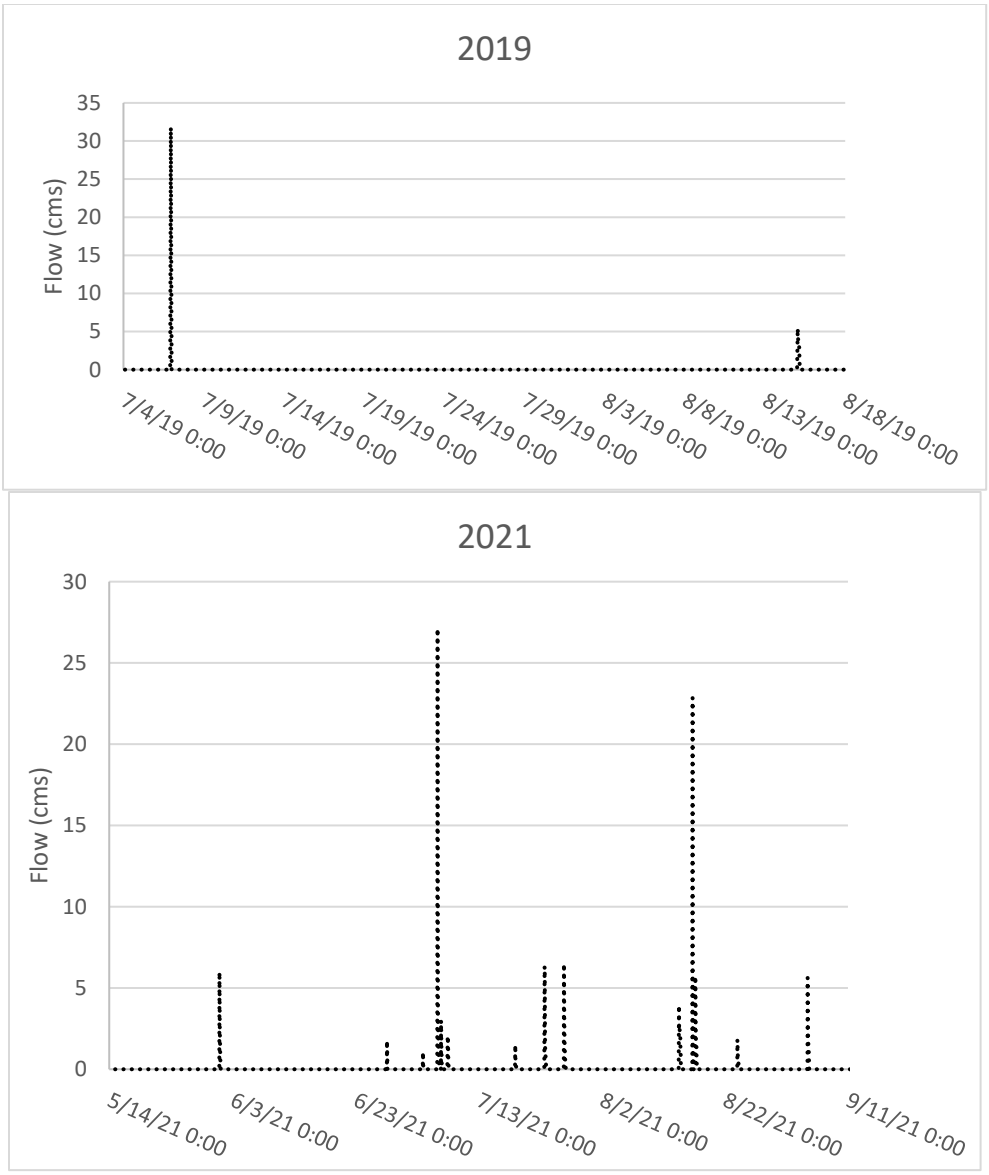

Two flow events were recorded in 2019 with peak flow rates of 31.8 and 10.0 m^3/s (cubic meters per second). At least 11 separate events were recorded in 2021 with peak flow rates ranging from 1.1 to 27.1 m^3/s (Table 4). Two years of peak flow data are not enough to determine design storm peak flows based on observations alone and are not sufficient to validate the estimated peak flow presented in Table 3 (Section 2.7).

Table 4. Observed peak flow values for individual events in 2019 and 2021.

Year	Date, Time (Zulu)	Obs Peak Flow (m^3/s)
2019	06 Jul 2019, 23:00	31.8
	15 Aug 2019, 01:00	10.0
2021	31 May 2021, 22:00	6.0
	28 Jun 2021, 03:00	1.8
	03 Jul 2021, 23:00	1.1
	06-07 Jul 2021, 08:00	27.1
	18 Jul 2021, 23:00	1.5
	23 Jul 2021, 17:00	6.3
	26 Jul 2021, 21:00	6.5
	14 Aug 2021, 13:00	3.9
	16 Aug 2021, 18:00	22.9
	24 Aug 2021, 01:00	1.8
	04 Sep 2021, 11:00	5.6

On 7 July 2021 at 17:00 local time (22:00 Zulu), ITAM staff observed an active flood event at the Thurgood main channel (culvert 1) and the first culvert to the south (culvert 2). Flow observations from the HOBO samplers indicate flow in the main channel was approximately 2.0 m^3/s (see Figure 18). Due to the short duration of flow events at the study site, this was the first time flow had been witnessed and documented in person.

Figure 18. 7 July 2021 flood event at downstream gauge station (*top left*), upstream face of culvert 1 (*top right*), culvert 2 looking upstream (*bottom left*), and culvert 2 looking downstream (*bottom right*).

3.2 Sediment load estimates

3.2.1 Bedload field measurements

When the four pit trap samplers were installed, composite samples were collected from the excavated material (substrate samples). The particle size distributions for upstream and downstream substrate samples are shown in Figure 19. The upstream samples have a larger average particle size than the downstream location, and the sample spread is lower. The downstream sample spread is large. The quantity of large particles at the base of the canyon (just upstream of the fan apex) is significant, so larger particles are more likely to be numerous at the upstream sampling location. Some larger particles make it downstream, resulting in a wider particle mixture near RR7.

Figure 19. Native bed substrate samples at pit traps 1 and 2 (upstream, *top*) and 3 and 4 (downstream, *bottom*) locations.

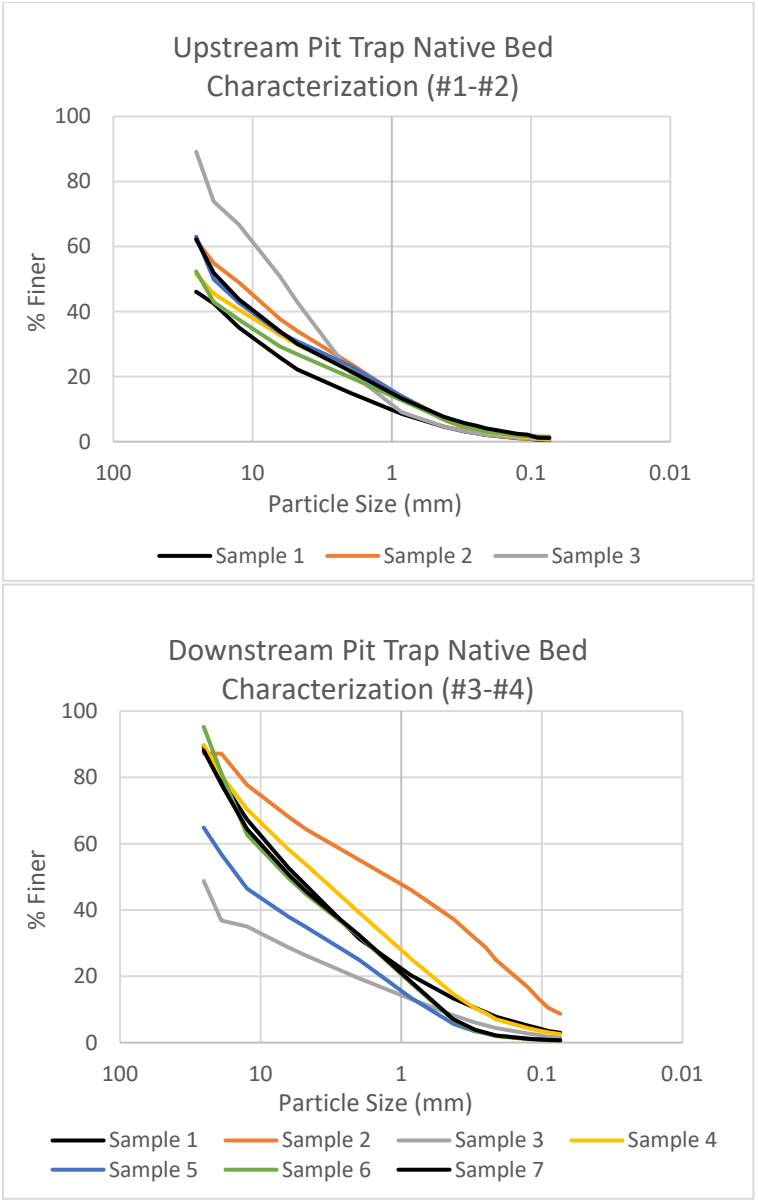

Samples were collected from pit traps 2–4 following the 6 June 2019 and 5 September 2021 events (Figure 20). No discernable pattern in particle sizes could be determined between the upstream and downstream locations or with regards to the pit trap locations within the channel, but the particle size difference between the events is large. The 6 June event had a peak flow of 31.8 m^3/ss, compared to a significantly smaller peak of 10.0 m^3/s during the 5 September event. The average particle size difference between each trap was 290%, 320%, and 180% for traps 2, 3, and 4, respectively (Table 5). The large material that didn't pass the 25.4 mm (2

inch) sieve was measured by hand. The average large particle size from the upstream sample sites were medium cobbles, while the average particle size from the downstream sample sites were small boulders (Table 6). These results indicate that larger particles became mobile during the large flow event due to the greater flow energy, which is consistent with the literature.

Figure 20. Composite samples from all pit traps for 6 June 2019 event (*top*) and 5 September 2019 event (*bottom*).

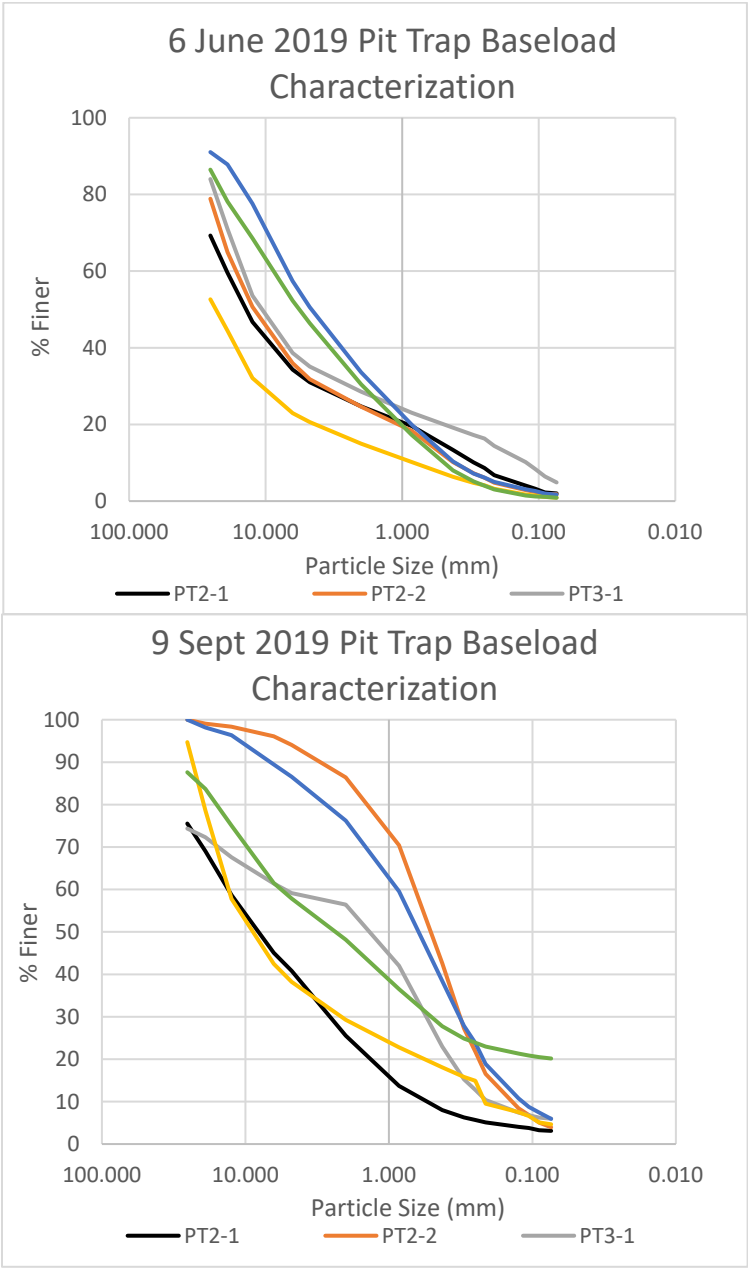

Table 5. Average sieve analysis material size by weight less than 25.4 mm.

Average Particle Size - Bed Material (mm)			
Location	Native Bed	6-Jul-19	9-Sep-19
Pit Trap 1	10.51	-	-
Pit Trap 2	9.19	13.19	4.56
Pit Trap 3	17.38	17.18	5.43
Pit Trap 4	21.02	5.2	2.9

Table 6. Average material size for material not passing the 25.4 mm sieve.

Sample Location	Average Particle Size above 25.4 mm
Pit trap 1 (Upstream)	Medium cobble (64–128 mm)
Pit trap 2 (Upstream)	Medium cobble (64–128 mm)
Pit trap 3 (Downstream)	Small boulder (>256 mm)*
Pit trap 4 (Downstream)	Small boulder (>256 mm)*

Large pit trap samplers were utilized on the Thurgood fan to capture a representative particle size distribution and to estimate total baseload. Evidence from the 2019 and 2020 sampling seasons indicate that the 5-gallon bucket traps were not large enough to do either. The July 2019 event moved a large amount of material with large individual particles. The single event buried pit trap 1, which was never recovered. The other pit traps were all buried during the beginning of the 2020 sampling season. Since the traps were filled during each event, the total bedload could not be estimated by direct field measurements.

Excessively large materials were moved during the July 2019 event that could not have been collected in the pit traps. Figure 21 shows the downstream HOBO location after installation in May 2019 and the same location following the July 2019 event. A large boulder (0.4 × 0.4 × 1 m) came to rest next to the HOBO following the July 2019 event. Such large particles were mobile during the event but could not have been collected in the pit traps, indicating that the pit traps underestimated the particle distribution.

* Some very large particles left at site (not measured).

Figure 21. Downstream HOBO and ISCO sampling location (2019–2020) in May 2019 (*top*) and following the July 2019 event (*bottom*).

3.2.2 Downstream bed surface deposition

Bed surface particle sizes were analyzed upstream and downstream of RR7, while composite sieve analyses were completed for the downstream

sites only. Results indicate that finer (sand) particle size decreases further downstream from RR7, which suggests that coarser sand particles drop out of the flow first after passing through the RR7 culvert (Figure 22). The average particle size by weight decreases downstream of RR7 (Table 7). The results indicate that the flow begins to lose energy just downstream of RR7.

Figure 22. Composite sample streambed surface distribution downstream of RR7.

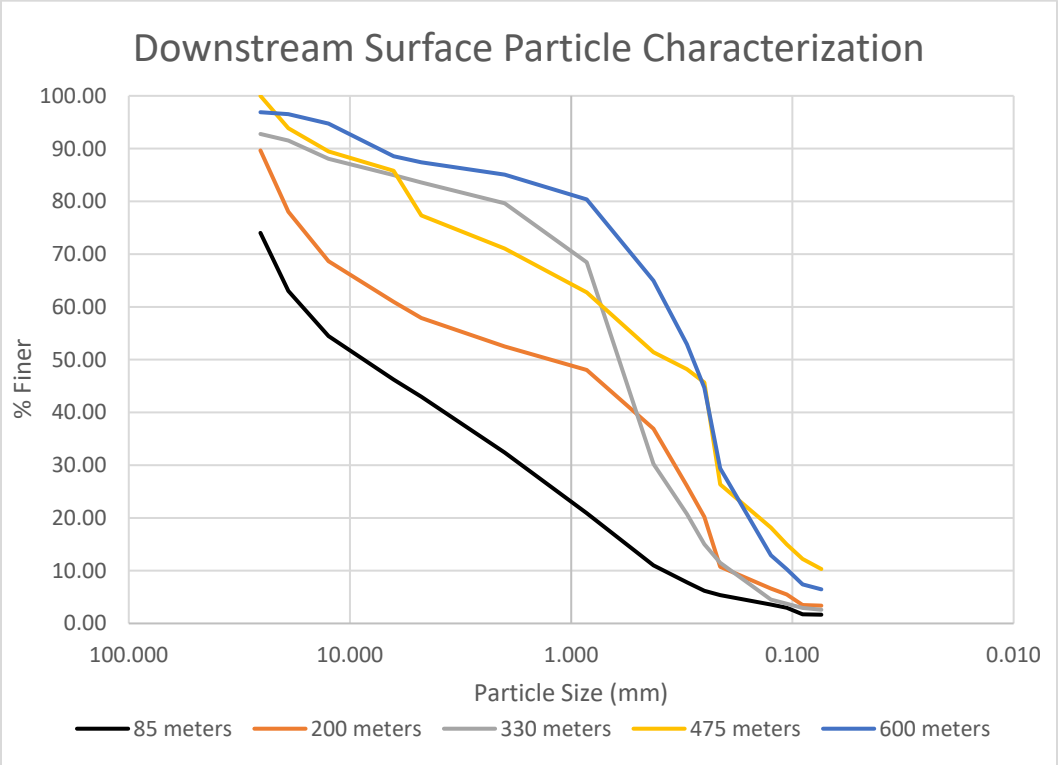

Table 7. Average sieve analysis material size by weight less than 25.4 mm downstream of RR7.

	Average particle size
85 meters	9.159 mm
200 meters	1.356 mm
330 meters	0.645 mm
475 meters	0.370 mm
600 meters	0.270 mm

The average bed surface large particle size from sample boxes A–N is provided in Table 8. Most of the sites had an average particle size of medium cobbles, while two sites averaged boulder-sized particles. These sites were just upstream of RR7 (consistent with samples from pit traps 3 and 4) and at the point where the channel becomes unrestricted (approximately

475 m downstream of RR7). These findings indicate that significant flow energy is lost at these locations resulting in the deposition of large base-load particles in these areas.

Table 8. Average bed surface material size for material not passing the 25.4 mm sieve.

Sample Location		Avg Particle Size above 25.4 mm
Upstream of RR7	250 meters (M&N)	Medium cobble (64–128 mm)
	130 meters (K&L)	Small boulder (>256 mm)
Downstream of RR7	85 meters (I&J)	Medium cobble (64–128 mm)
	200 meters (G&H)	Medium cobble (64–128 mm)
	330 meters (E&F)	Medium cobble (64–128 mm)
	475 meters (C&D)	Medium bolder (>381 mm)
	600 meters (A&B)	Medium cobble (64–128 mm)

3.2.3 Bedload modeling estimates

Bedload could not be measured directly with the pit traps but was estimated at the fan apex using Wilcock and Crowe (2003) (Figure 23). Surface and substrate particle size distributions, survey data, and hydraulic model outputs provided all required equation inputs. Calibration was not possible due to the lack of observable bedload data.

Figure 23. Bedload transport rate estimate at fan apex for range of anticipated flow rates.

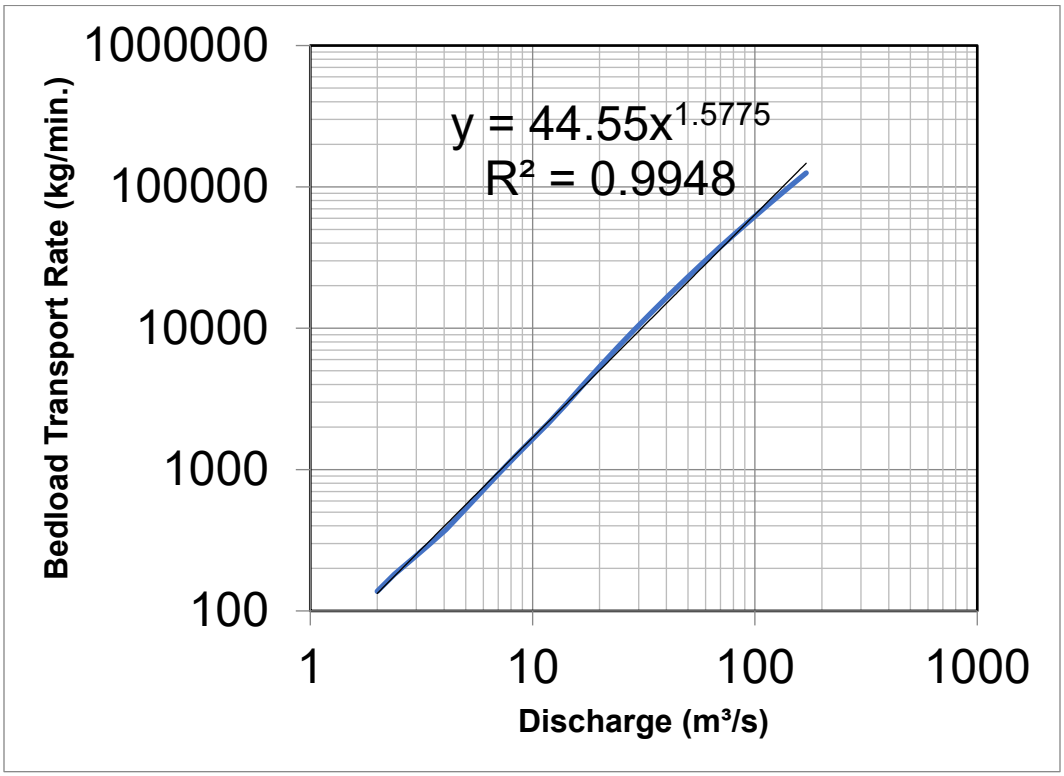

3.2.4 Suspended sediment measurements

Total suspended sediment samples were collected by the upstream ISCO sampler on 6 July 2021 and collected by the downstream sampler on 6 July 2019, 28 June 2021, 6 July 2021, and 4 September 2021. The two events on 6 July (2019 and 2021) were larger events with peak flows rates of approximately 32 m^3/s and 27 m^3/s, respectively. The other two events were smaller, with peak flow rates of 1.75 m^3/s on 28 June and 5.6 m^3/s on 4 September. The larger events produced much higher peak and average total suspended solid (TSS) concentrations than the two smaller events (Table 9, Table 10, Table 11, and Table 12).

The 6 July 2019 and 28 June 2021 sampling events captured the entire hydrographs as sampling terminated when the samplers could no longer detect flow. All 24 available bottles were filled during the 4 September 2021 event, which spanned all but 3 hours of the flow event. The samplers malfunctioned due to clogged intake lines during the 6 July 2021 event, so samples were not taken during the latter 5.5 hr of the flow despite available sample bottles. Only one sampler recorded each event due to clogged intake lines or failure of the unactivated sampler to detect flow. Numerous other flow events recorded by the HOBO loggers were not sampled by either sampler due to the same issues.

Table 9. Suspended sediment sample results 6 July 2019 event (downstream sampler).

Suspended Sediment Samples (6 July 2019)		
Sample Bottle	Sample Time (Zulu)	TSS (kg/m^3)
10	16:40	31.01
11	16:50	27.23
12	17:00	23.92
13	17:10	32.84
14	17:20	35.84
15	17:30	24.31
16	17:40	35.32
	Average (kg/m^3)	30.07
	Peak Flow (m^3/s)	31.78

Table 10. Suspended sediment sample results 28 June 2021 event (downstream sampler).

Suspended Sediment Samples (28 June 2021)		
Sample Bottle	Sample Time (Zulu)	TSS (kg/m^3)
2	2:27	15.24
3	2:37	9.41
4	2:47	7.51
5	2:57	6.68
6	3:07	5.53
7	3:17	3.76
8	3:27	4.58
9	3:37	4.73
10	3:47	4.73
11	3:57	4.19
12	4:07	4.28
13	4:17	3.89
14	4:27	3.98
15	4:37	3.63
16	4:47	3.21
	Average (kg/m^3)	3.86
	Peak Flow (m^3/s)	1.75

Table 11. Suspended sediment sample results 6 July 2021 event (upstream sampler).

Suspended Sediment Samples (6 July 2021)		
Sample Bottle	Sample Time (Zulu)	TSS (kg/m^3)
2	7:20	37.38
3	7:30	31.43
4	7:40	27.80
5	7:50	41.03
6	8:00	41.88
7	8:10	19.91
	Average (kg/m^3)	26.74
	Peak Flow (m^3/s)	27.11

Table 12. Suspended sediment sample results 4 September 2021 event (downstream sampler).

Suspended Sediment Samples (4 Sept 2021)		
Sample Bottle	Sample Time (Zulu)	TSS (kg/m³)
1	10:57	7.17
2	11:07	4.09
3	11:17	2.50
4	11:27	1.83
5	11:37	1.90
6	11:47	2.05
7	11:57	0.99
8	12:07	0.90
9	12:17	0.77
10	12:27	0.76
11	12:37	0.76
12	12:47	0.82
13	12:57	0.68
14	13:07	0.53
15	13:17	0.42
16	13:27	0.43
17	13:37	0.41
18	13:47	0.38
19	13:57	0.36
20	14:07	0.36
21	14:17	0.37
22	14:27	0.37
23	14:37	0.36
24	14:47	0.44
	Average (kg/m³)	0.38
	Peak Flow (m³/s)	5.62

Observed streamflow data and the TSS data were used to determine total suspended sediment loads during the four sampled flow events (Table 13).

Table 13. Total suspended sediment load per sampled flow event.

Events	Peak Flow (m³/s)	TSS per Event (MT)
6 Jul 19	31.78	2046
28 Jun 21	1.75	47
6 Jul 21	27.11	2411*
4 Sep 21	5.62	31.1
		*Partial value

3.2.5 Total sediment load

Total sediment load for 2019 and 2021 was estimated using observed streamflow data as well as the bedload and suspended sediment load transport rates (Table 14). Upper and lower bounds are provided due to assumptions made about individual event hydrographs at subhourly timesteps and due to the limited number of TSS sampling events.

Table 14. 2019 and 2021 sediment loads from Thurgood Canyon given as upper and lower bounds.

Calendar Year	Bedload (MT)	Suspended Load (MT)	Total Sediment Load (MT)
2019	325–400	1,800–2,250	2,125–2,650
2021	1,025–1,200	4,000–5,200	5,025–6,400

Arid alluvial fans are episodic, so the total volume of water and sediment moved year to year vary significantly depending on the number and magnitude of events.

3.3 GIS and lidar assessments

The GIS study area ranges from the alluvial fan apex to Salt Creek. Slope, watershed, and preferential flow path assessments were completed using the 2019 topographic data set for most of the fan, while additional analysis focuses on four study areas, as seen in Figure 24. The DEM analysis covered the change over time between 2013 to 2019 and 2019 to 2021. Note, the 2021 DEM did not cover the area near Salt Creek. The vegetation analysis covered the change over time between 2011 and 2020. These two methods combined give a picture of where water is flowing through the fan and how the RR7 culvert and main channel berm impact this flow.

Figure 24. The study areas are located upstream of RR7 (*red box*), downstream of RR7 (*green box*), at the culvert south of the bridge (*blue box*), and downstream near Salt Creek (*purple box*).

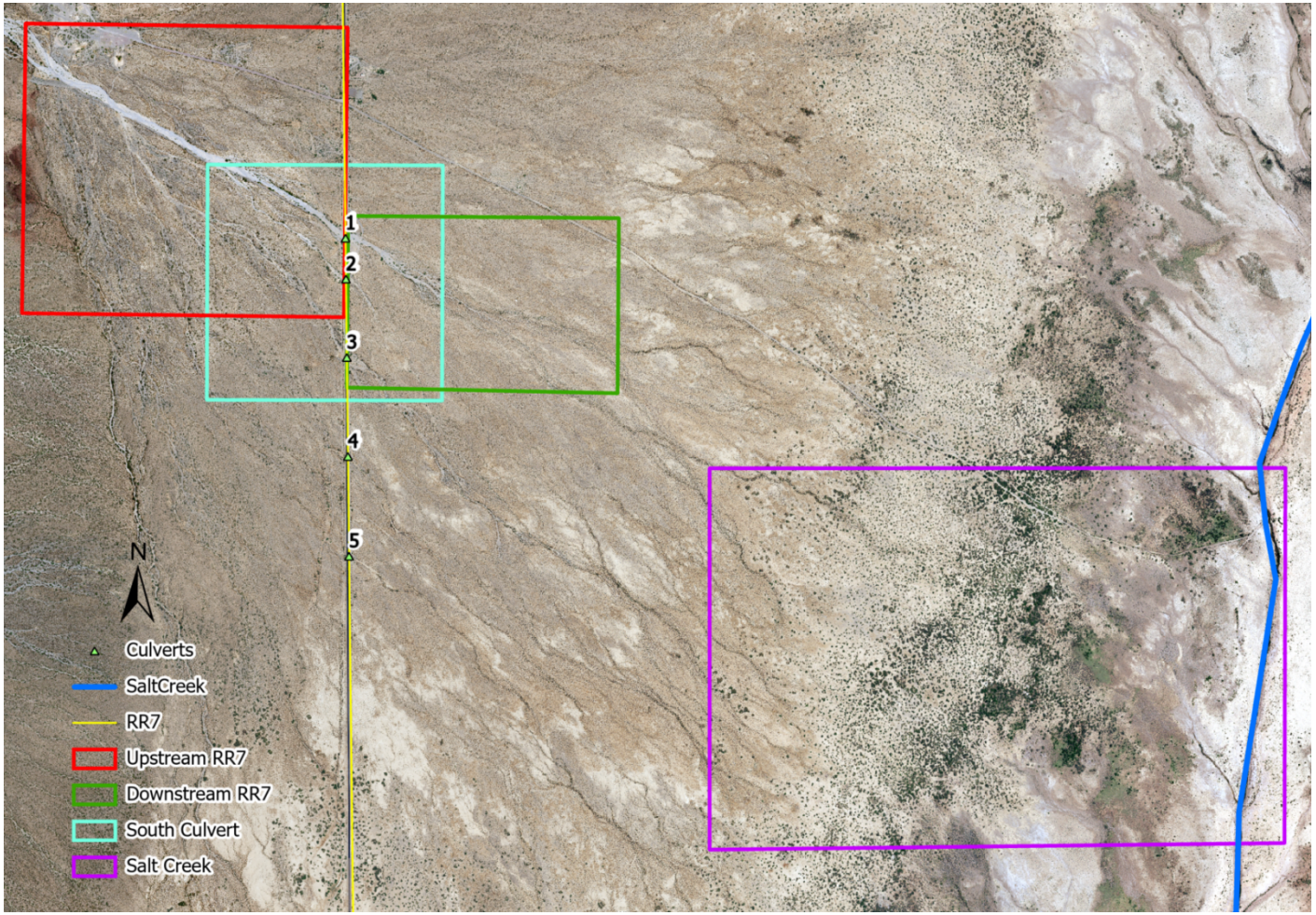

3.3.1 Salt Creek and the alluvial fan base

Vegetation is more numerous, with greater coverage, within 2 km of the west side of Salt Creek compared to further up the fan (Figure 25). The relative abundance of vegetation may be due to greater water availability near Salt Creek as a result of a higher water table near the valley floor.

Figure 25. 2011 (*top*) and 2019 (*bottom*) aerial photos of the heavy vegetation area near Salt Creek (*purple box* in Figure 25).

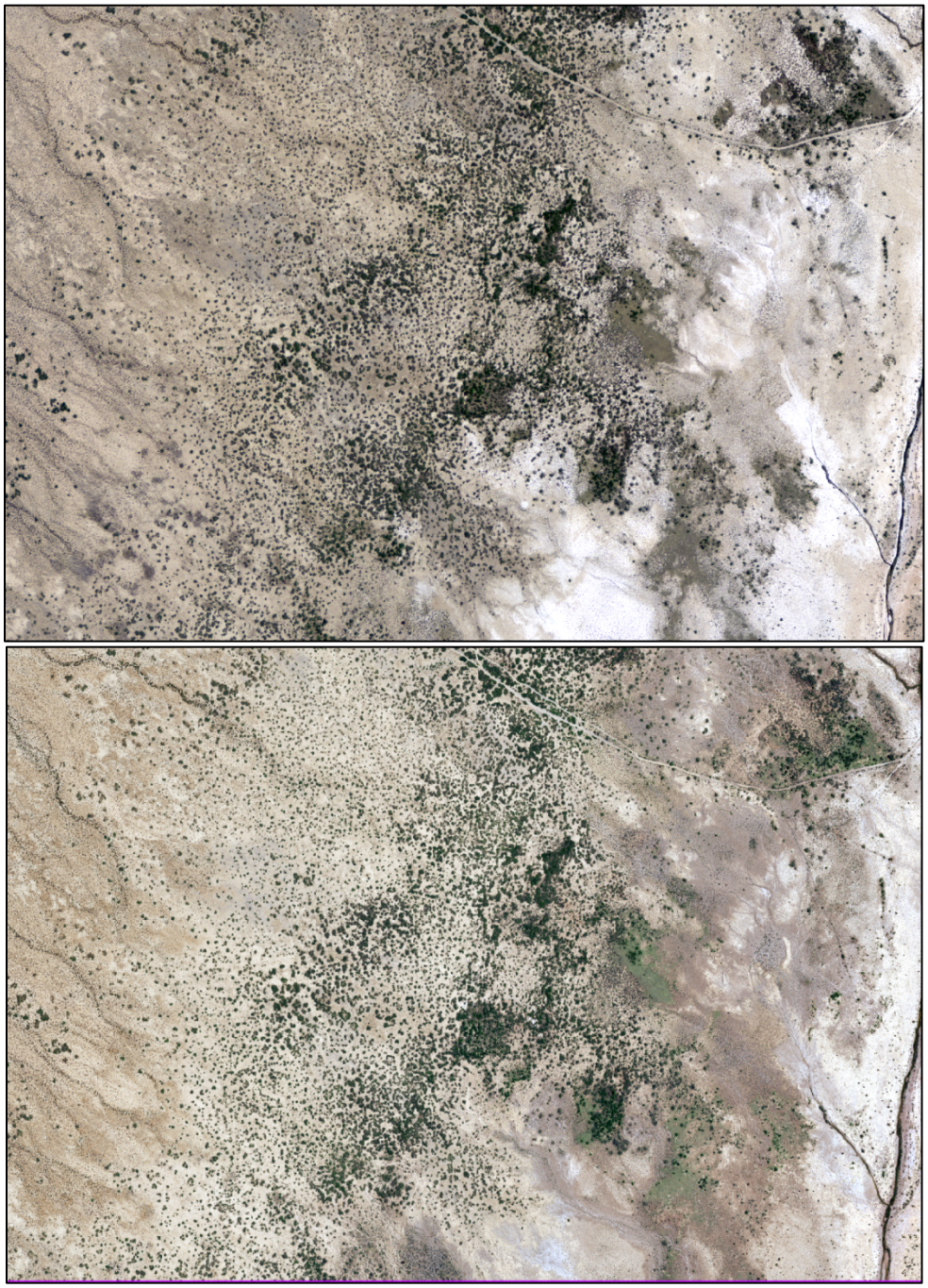

DEM comparisons between 2019 and 2013 of the lower fan show no apparent changes to the fan surface or to existing or developing channels from the main channel, indicating Thurgood Canyon drainage did not affect Salt Creek directly during the 2013–2019 time frame (Figure 26). Channelization caused by flow from the main drainage channel can be seen in the northwest corner of Figure 26; however, it fades starting around 2.6 km from RR7 and no changes in channels can be detected starting about 3 km downstream of RR7.

Figure 26. 2019 DEM minus 2013 DEM just west of Salt Creek (*purple box* in Figure 25). Salt Creek is on the *right* (*blue*). The *red line* indicates where fan channels end about 3 km from RR7.

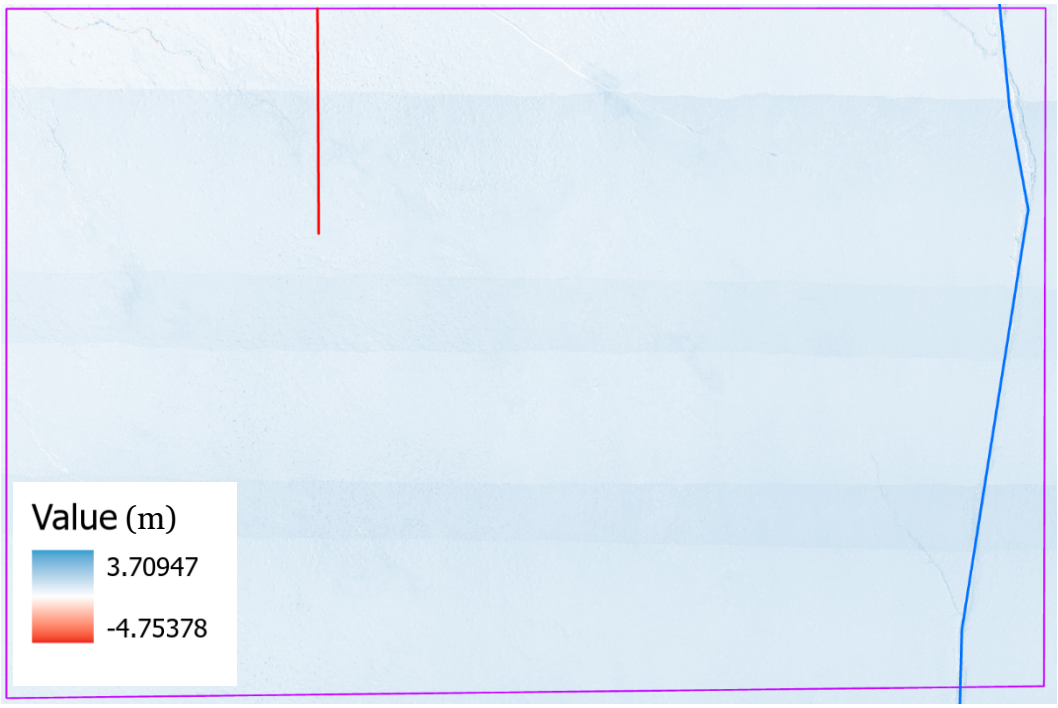

The NDVI difference between 2020 and 2011 of the lower fan shows no evidence of vegetation loss due to scour or changes to the land surface, so no figure is shown.

3.3.2 Just downstream of RR7

Downstream of RR7, the main drainage channel for Thurgood Canyon becomes unrestricted because the berms upstream of RR7 do not extend further east. The main channel remains channelized for about 500 m before bifurcating into smaller channels (Figure 27). This area is also characterized by a debris field of sediment, including sand, cobbles, and much

larger particles. As the single, large channel begins to fan out into numerous channels, the flow loses sediment carrying capacity and the suspended sediment falls out of the flow and deposits in this area. These significant sediment deposits cause preferred flow paths (channels) in this area to change from flow event to flow event. New channels can be scoured out, while channels utilized during the previous event can be filled back in.

Figure 27. 2011 (*top*) and 2019 (*bottom*) aerial photos just downstream of RR7 (*green box* in Figure 25).

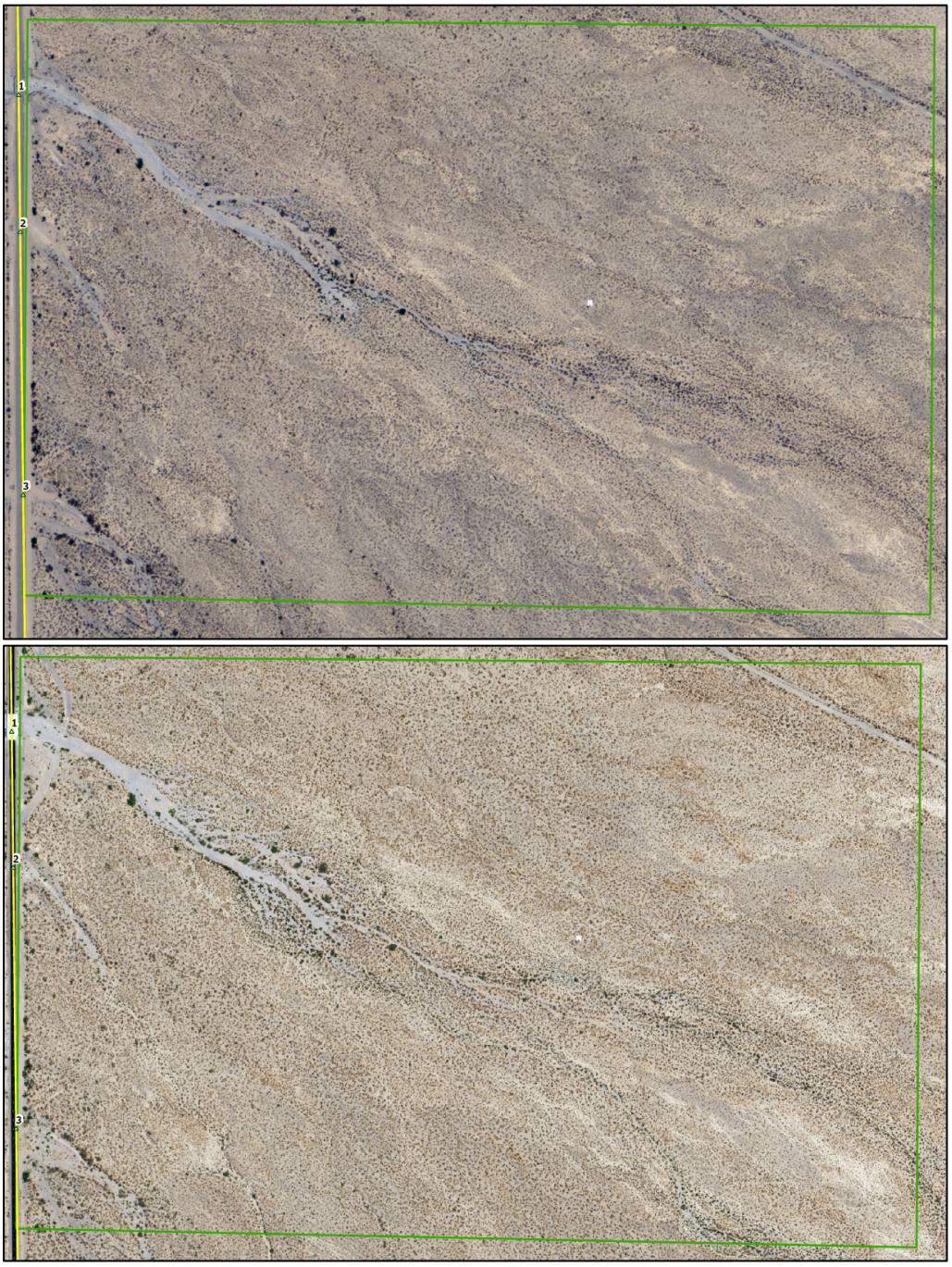

Downstream of the RR7 box culvert, there is a moderate amount of deposition seen in the main channel before flow spreads into numerous smaller channels downstream (Figure 28). The areas of deposition and the preferred flow path (channel) development can be seen over the two periods. Minor flows through the channels causes deposition in some old channels, while major flows cause the water to travel much further southeast and create or enlarge new channels. As noted above, these overland channels do not extend more the 3 km downstream of RR7.

Figure 28. 2019 DEM minus 2013 DEM (*top*) and 2021 DEM minus 2019 DEM (*bottom*) just downstream of RR7 (*green box* in Figure 25).

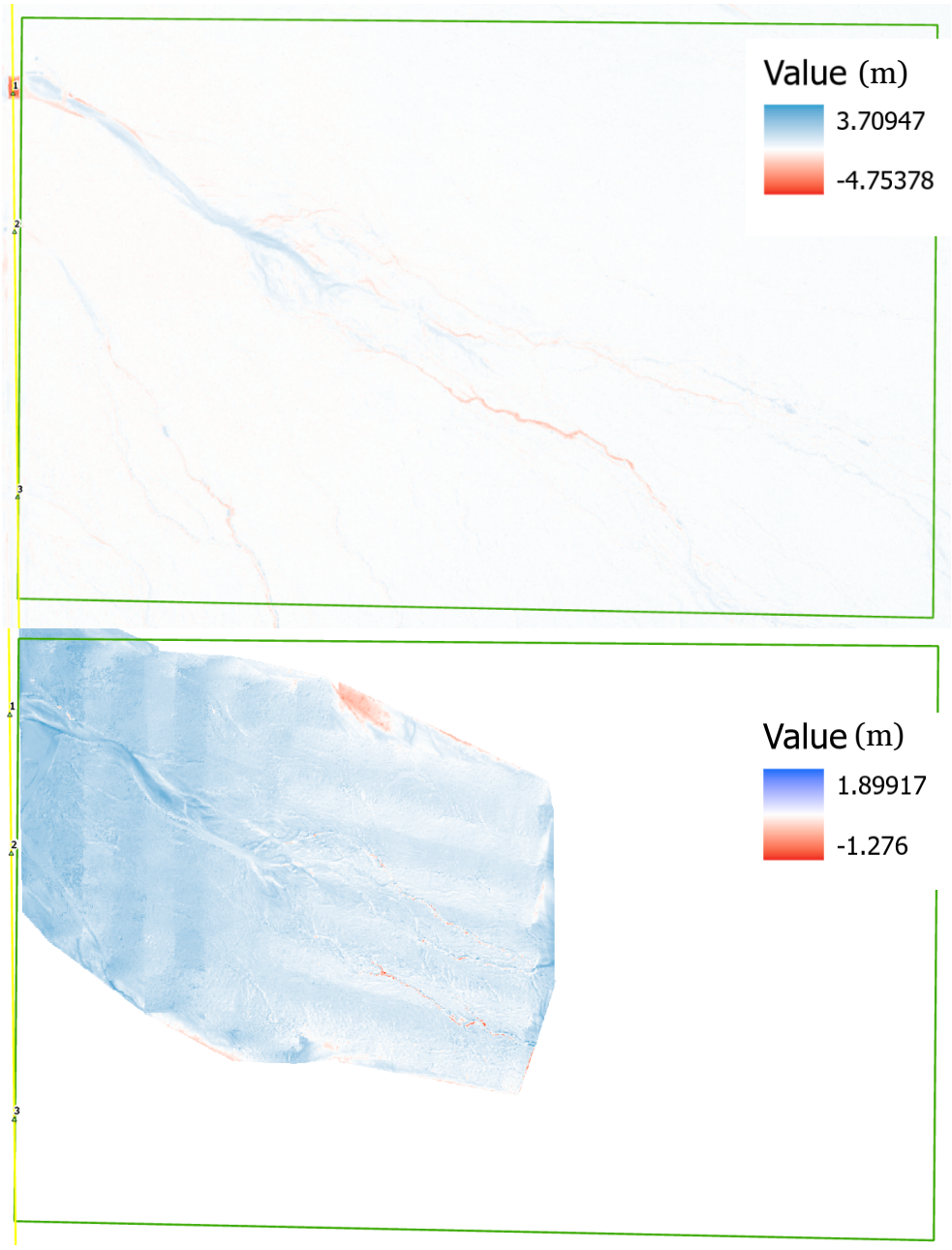

The NDVI analysis reveals a similar trend of deposition immediately after RR7 where the abundance of moisture and new sediment promotes vegetation establishment and healthy growth. Some scouring and channel formation starting approximately 400 m downstream of RR7 are seen as reflected by the loss of vegetation along scoured channel banks (Figure 29). There is an increase of vegetation where water is plentiful, and erosion is observed to be low after the road. Channels of *red* with *green* edges appear further downstream indicating erosion of channels and water availability to foster vegetation growth at the edges of those channels.

Figure 29. NDVI difference between 2020 and 2011 just downstream of RR7 (*green box* in Figure 25).

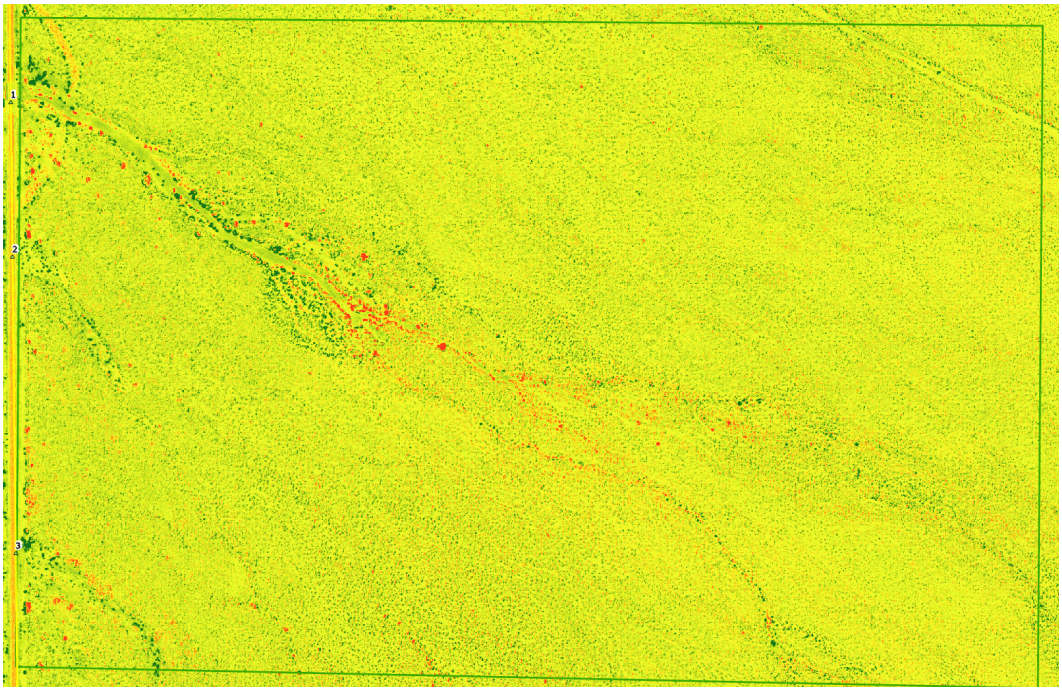

3.3.3 Upstream of RR7

The main channel upstream of culvert 1 experiences the most concentrated flow on the fan. Due to the primary berm on the south bank, most of the flow from Thurgood Canyon runs through this channel and into culvert 1. Scour occurs frequently along this channel, particularly along the primary berm (Figure 30).

Figure 30. 2011 (*top*) and 2019 (*bottom*) aerial photos of the main upstream channel (*red box* in Figure 25).

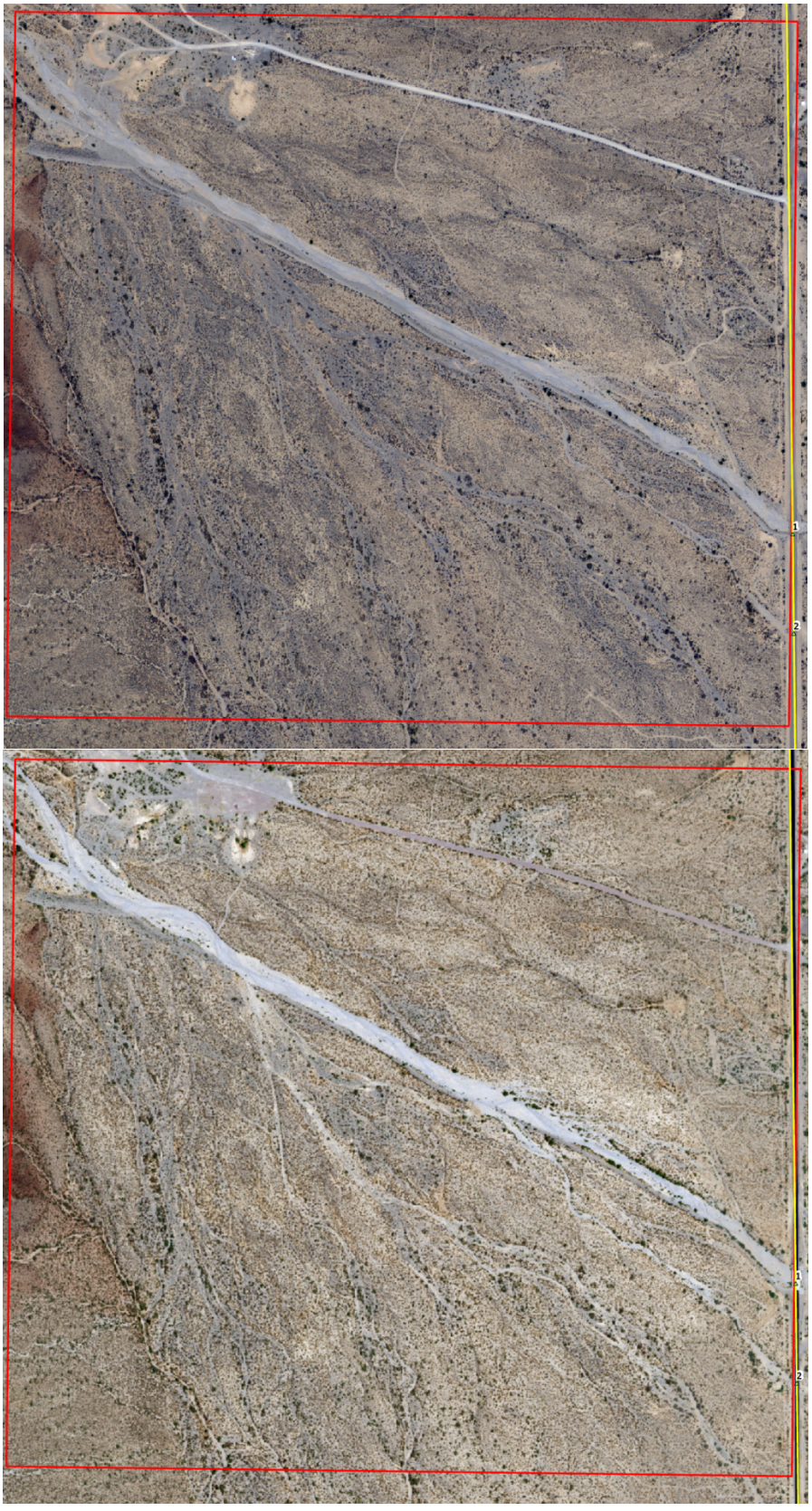

When comparing 2019 to 2013 and 2021 to 2019, four scour locations along the main channel's south berm were detected. In addition, a few areas of concentrated deposition can be seen along the edges of the main channel. There is a general trend of deposition in the middle of the channel with scour occurring on the edges. A secondary channel originating at the fourth (downstream) berm scour location and heading towards culvert 2 can be seen in both DEM comparisons. A portion of the flow in the main channel left through the fourth scour hole and enlarged the secondary channel heading to culvert 2. Areas of deposition also occurred near the fourth scour hole.

In addition to the fourth scour hole, the second scour hole (from the upstream end) is large enough to allow discharge in the main channel to flow to the south. The aerial images show historic channels at this location (Figure 31), but the DEM comparisons fail to detect the changes of the nearby secondary streams. The flow in this area most likely traveled down existing secondary channels and was of too low energy to cause moderate to significant scour and create new preferred flow paths.

Figure 31. 2019 DEM minus 2013 DEM (*top*) and 2021 DEM minus 2019 DEM (*bottom*) just upstream of RR7 (*red box* in Figure 25).

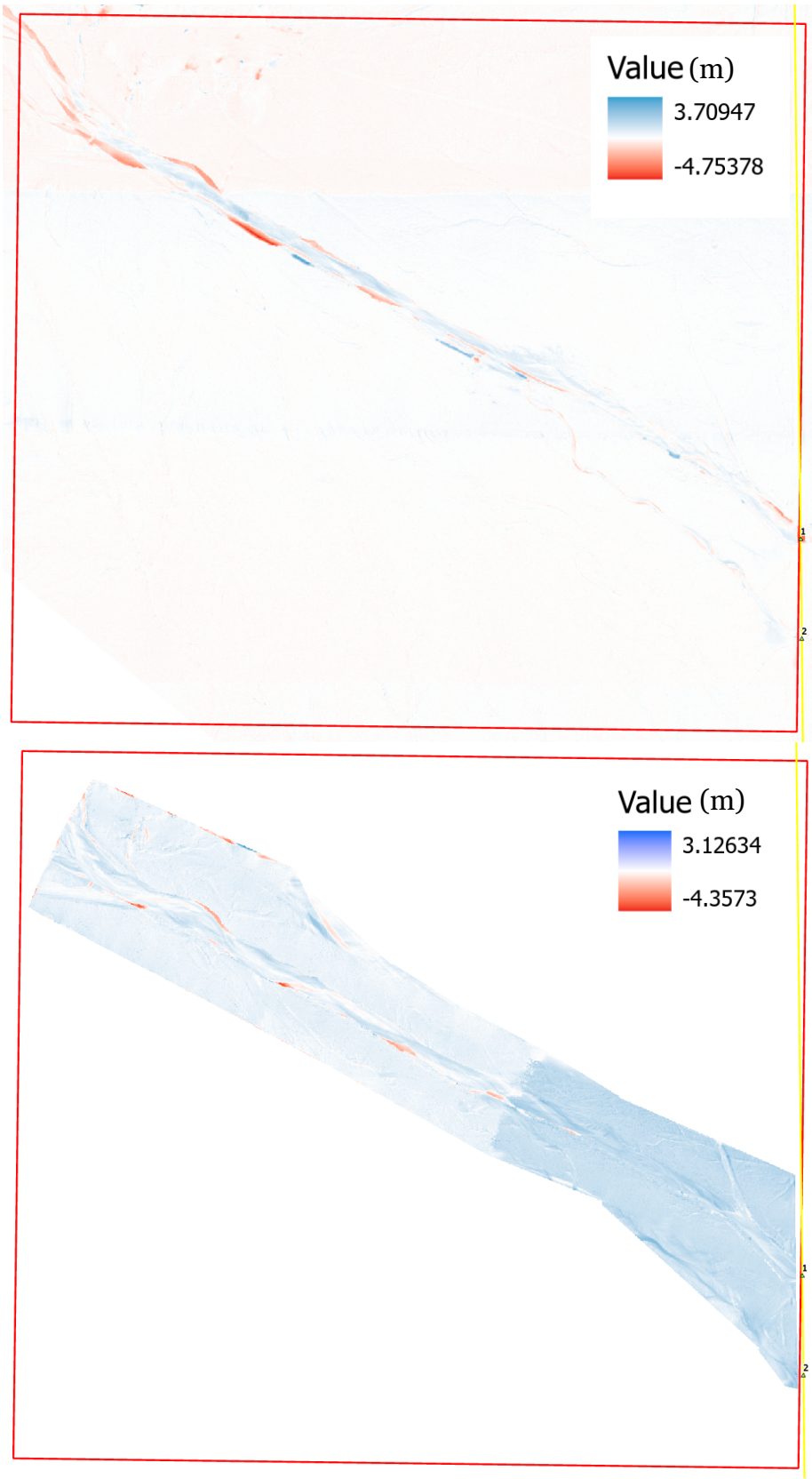

There is noticeable vegetation growth at the edges of the main channel near RR7 (Figure 32) as well as some areas of vegetation loss much further upstream on the north side berm. Changes in vegetation can also be seen along the secondary channel leading from the fourth scour location to culvert 2. Increases in vegetation are likely due to more plentiful water from overflows, while individual plants were lost along the channel edge due to scour.

Figure 32. The difference in NDVI between 2020 and 2011 upstream of RR7 (*red box in Figure 25)*.

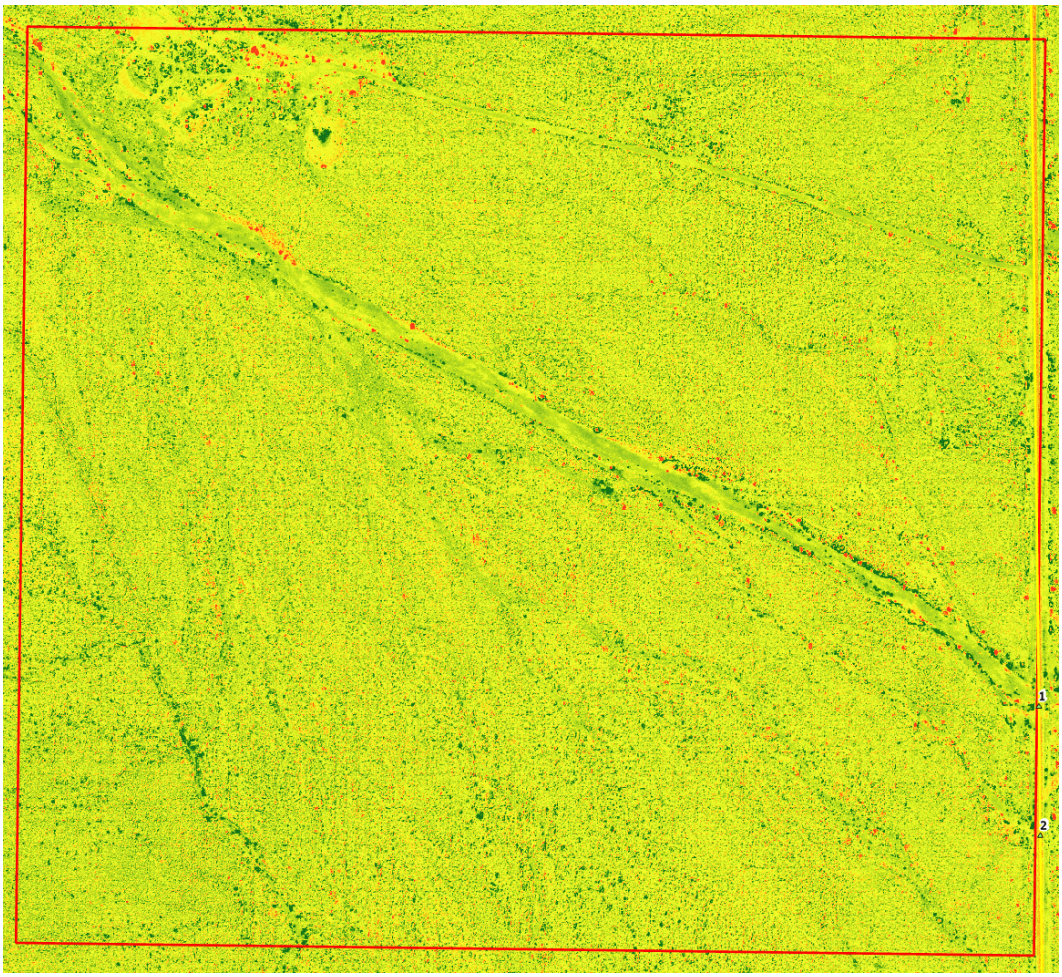

3.3.4 Southern section of Thurgood alluvial fan

As noted in Section 3.3.3 , significant scour has occurred at four points along the primary main channel berm between the fan apex and RR7 (Figure 31). Scour locations 1–4 (from upstream to downstream) become larger during successive significant flow events. As of March 2022, scour holes 2 and 4 could allow overflow to the south during small flow events,

while scour hole 3 could allow overflow during moderate events (Figure 34). Flow from scour locations 3 and 4 currently go to culvert 2, while flow from scour location 2 may go to culverts 2, 3, and/or 5 depending on the preferential flow paths from event to event.

Figure 33. Thurgood Canyon alluvial fan detailing locations of berm scour, secondary drainage channels, secondary drainage divides, and culverts to the south of the main drainage channel.

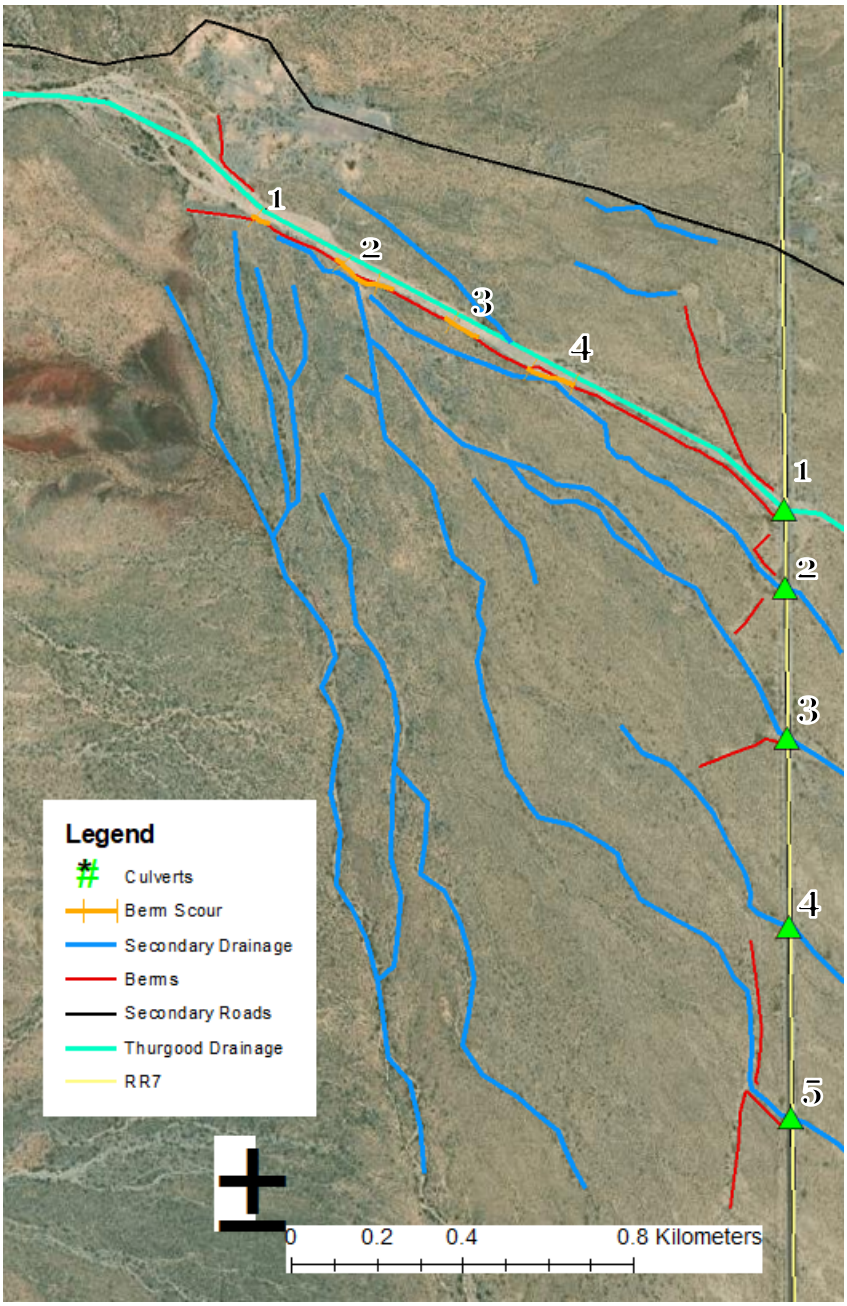

Figure 34. Scour locations 1–4 (starting *top left*, clockwise) as of March 2022.

The general preferential flow direction of overland flow leaving Thurgood Canyon seems to be towards the south and southeast as judged by historic drainage channels and present-day berm scour locations. To determine the general alluvial fan slope in multiple directions, 19 profile lines were cut from the fan apex to the fan base and the average slopes were calculated from the 2019 DEM (Figure 35). The average slope of the fan is highest to the south (profile A) and decreases as the profiles move northeast (Table 15). If the current flow control BMPs were removed, most of the runoff from Thurgood Canyon would flow from the fan apex in a southern direction.

Figure 35. Slope profiles A–S.

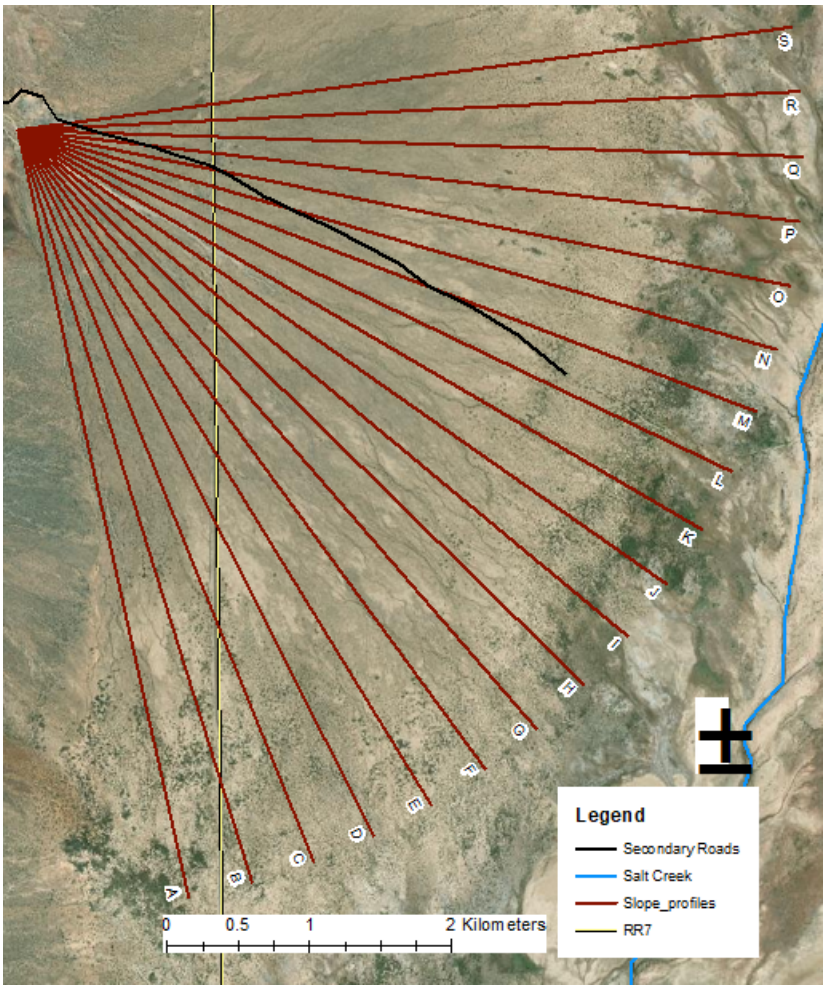

Table 15. Average slope of select profiles.

Profile	Average Slope (m/m)
A	0.017
F	0.0166
K	0.0163
P	0.0163
S	0.0152

Aerial images from 2011 and 2019 show growth of the secondary channel leading to culvert 2 (Figure 36). Channels leading to culverts 3 and 4 are also visible, but no significant changes can be detected from the images alone.

Figure 36. 2011 (*top*) and 2019 (*bottom*) aerial photos of culvert 2 south of the main channel (*blue box* in Figure 25).

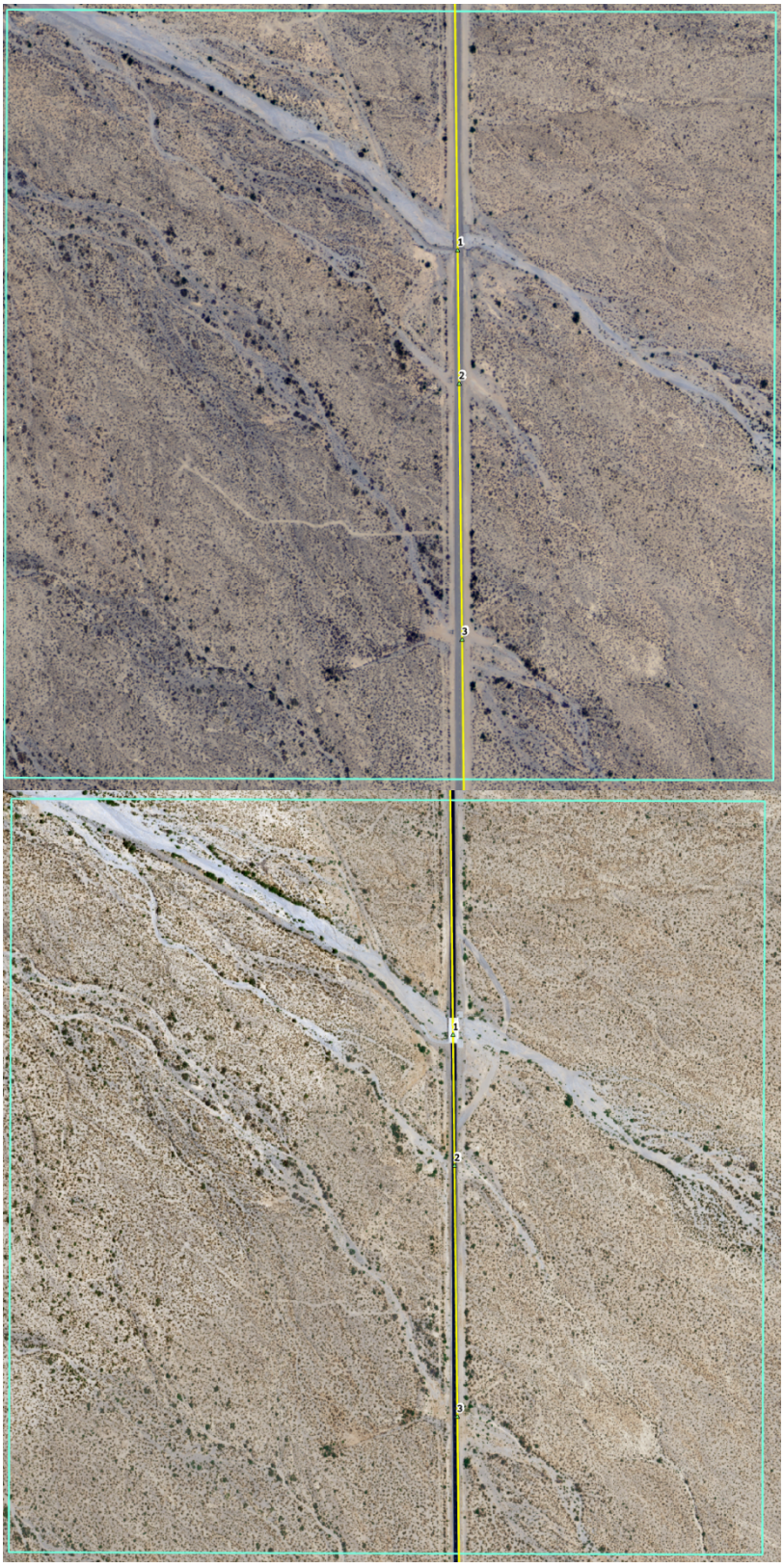

The DEM analysis in this area is only possible between 2013 and 2019 but has nonetheless shown scour along the secondary channel leading to culvert 2 (Figure 37). New channelization also occurred leading to culvert 4, but this new channel development does not extend all the way back to the main drainage channel, suggesting any overland flow in this area was the result of rainfall directly on the alluvial fan and not due to flow diverting from the main channel at scour location 2. In addition, Figure 31 shows no evidence that flow from scour hole 2 reaches any of the southern culverts.

Figure 37. Channelization occurring through the culvert south of the bridge (*blue box* in Figure 25).

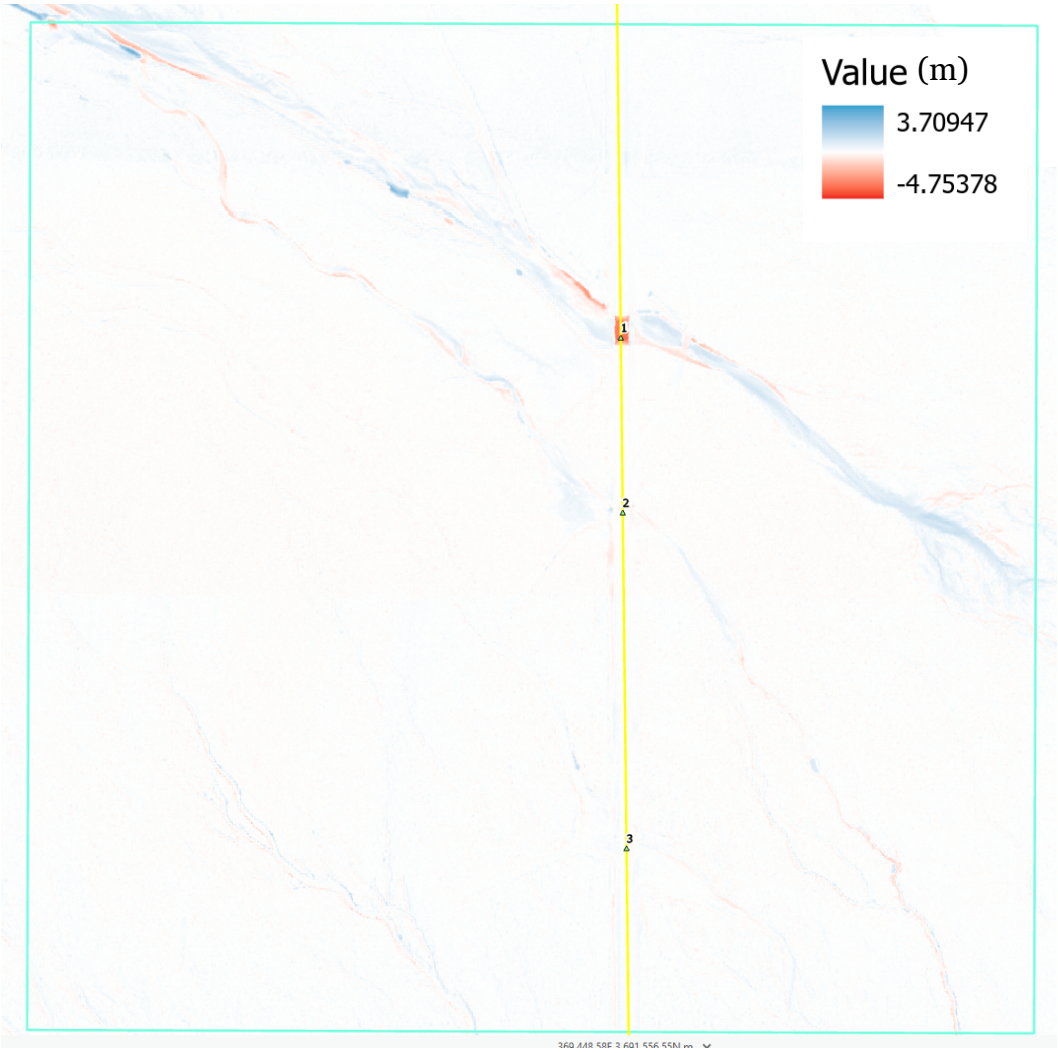

The NDVI assessment in Figure 38 shows increased vegetation establishment along the secondary channels leading to culverts 2–4, which is likely a result of more abundant moisture availability. However, no evidence of significant scour is detected.

Figure 38. NDVI difference between 2011 and 2020 around culverts 2 and 3, south of the main channel (*blue box* in Figure 25).

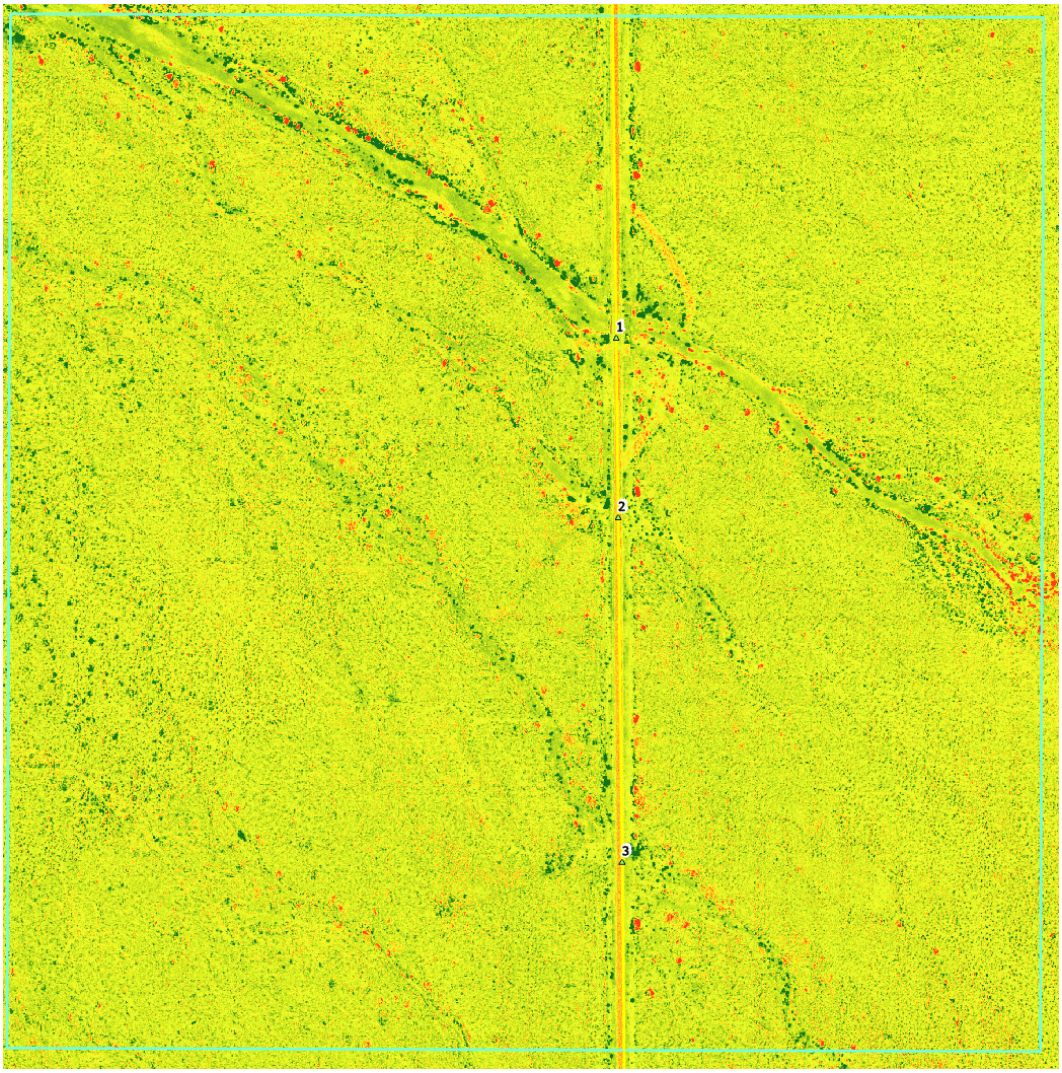

The GIS analysis indicates no detectible overland flow from Thurgood Canyon has reached Salt Creek since 2011. This is because the majority of water and sediment infiltrates or deposits within 3 km downstream of RR7. Upstream of RR7 the primary berm has been repeatedly scoured and rebuilt since at least 1996. A portion of the main flow currently leaves the main channel at two locations, flowing to culvert 2.

3.4 Hydrology

3.4.1 Calibration

The initial parameter sensitivity assessment for the Thurgood model indicated that the model underestimated peak flow events. Peak flow rates were most sensitive to hydraulic conductivity (saturated and unsaturated) and surface storage parameters. The ModClark parameters (time of concentration and storage coefficient) affect the timing, shape, and peaks of the hydrographs. Calibration was limited to these parameters.

Hydrologic model performance was assessed by graphical representation of the relationship between model simulations and observations as well as an absolute value error indicator. The absolute value error indicator was used because the flow events being compared were very short in duration, making the peak flow values the only point of comparison. We used the root-mean-square error (RMSE). Calibration was conducted by first adjusting hydraulic conductivity, then surface storage. Evaluation of the calibration was done graphically and statistically. Once these values were set, all combinations of the ModClark parameters were tested to determine the statistically optimal combination (minimized RMSE) across the parameter space.

Calibration and validation simulations were completed for June–October for 2021 and 2019, respectively. Minimum error between observed and simulated peak stream flow was achieved when Ko, Ks, ToC, and SC were 50% of their original values and surface storage was 25% of its original value (Table 16). The 2019 validation period supported the model calibration.

Table 16. RMSE for a range of ModClark parameter values for the 2021 calibration period and the 2019 validation period. RMSE units are m³/s.

2021	SC 0.05	SC 0.25	SC 0.5	SC 0.7	SC 0.9	SC 1.0
ToC 0.5	2.42	1.91	1.72	1.78	2.08	2.54
ToC 0.7	2.37	1.90	1.72	1.77	2.07	2.48
ToC 0.9	2.44	1.93	1.72	1.79	2.12	2.56
ToC 1.0	2.33	1.89	1.71	1.77	2.05	2.43
2019	SC 0.05	SC 0.25	SC 0.5	SC 0.7	SC 0.9	SC 1.0
ToC 0.5	2.41	1.93	1.75	1.80	2.11	2.56
ToC 0.7	2.38	1.93	1.75	1.80	2.09	2.52
ToC 0.9	2.51	2.01	1.80	1.87	2.20	2.66
ToC 1.0	2.34	1.92	1.74	1.80	2.07	2.48

The calibrated HEC-HMS model results and the observed hydrographs are provided in Figure 39. The model performance is mixed, overestimating peak flows in both the calibration and validation periods while also underestimating peak flows for other events. The model produces well-timed hydrologic responses for almost all observed events, regardless of size, indicating that the model produces runoff if forcing precipitation occurs in the basin. The observed hydrographs are very short in duration, usually less than 12 hours from start to finish, so the model must accurately convert excess rainfall to runoff. The mixed performance of the calibrated model is mostly likely due to the limitations of the Stage IV forcing data to accurately represent precipitation over the Thurgood basin. Since flood events in the basin are exclusively due to excess precipitation, the calibrated model is sensitive to the spatial variability and intensity of the gridded precipitation product. Modeled basins are less sensitive to the spatial and temporal accuracy of the precipitation when antecedent soil moisture or groundwater contribute significantly to the magnitude and timing of floods.

Figure 39. Calibration and validation hydrographs for 2021 and 2019, respectively.

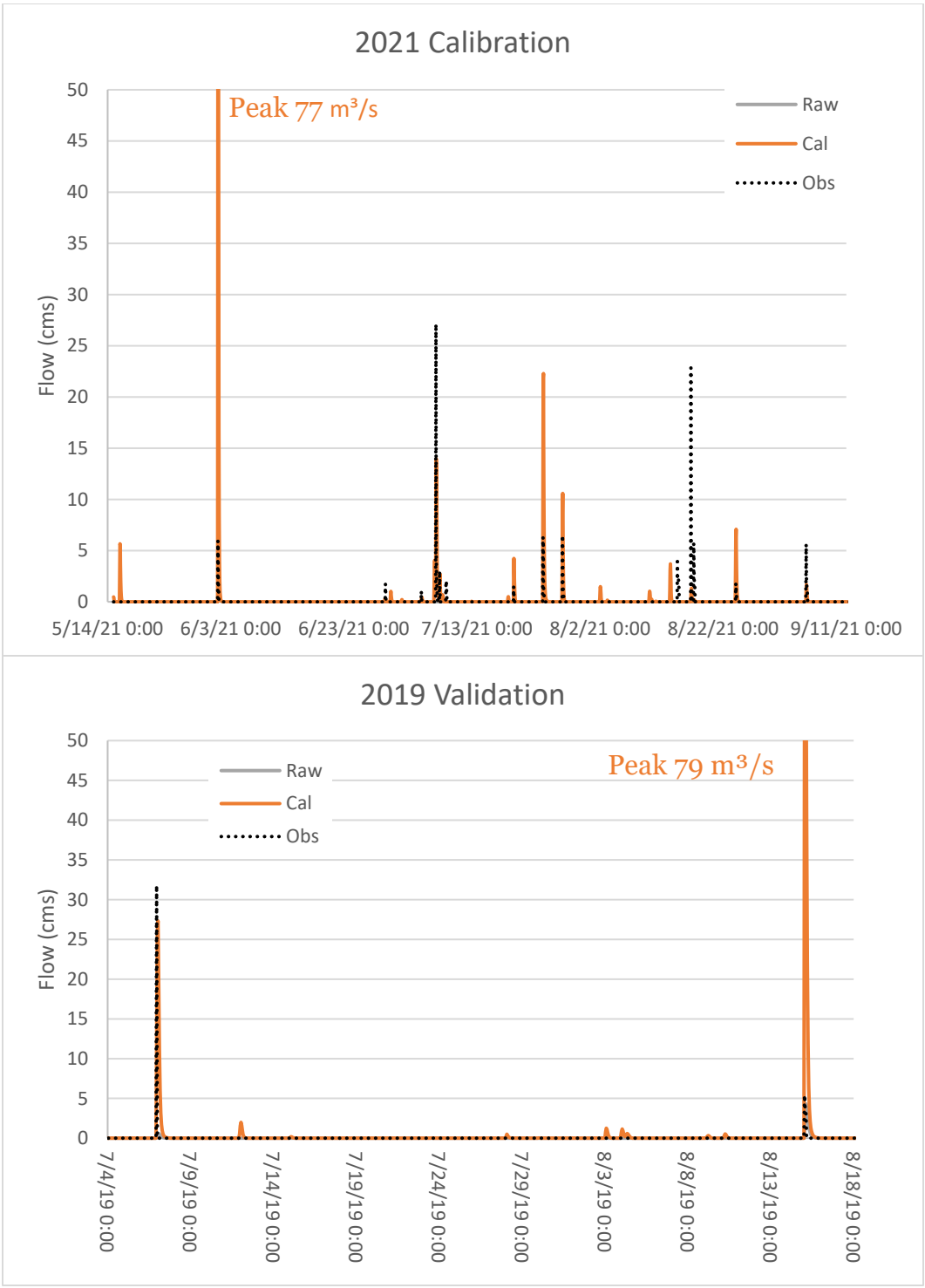

Despite limitations, the Thurgood HEC-HMS model can provide information on the approximate number and magnitude of flow events that occurred during the period 2013–2021, which overlaps with the DEM comparison study period.

3.4.2 2013–2021 flow analysis

There was at least one flood event per year greater than 20 m^3/s in Thurgood Canyon between 2013 and 2021 (Figure 40). The annual modeled maximum floods were between 25 and 100 m^3/s, with an average of 53 m^3/s. Based on the peak flow analysis by the USACE Tulsa District (Table 3), these peak flows represent events between 2 yr and 40 yr events according to regression equations, or less than the 10 yr event according to the previous modeling study.

Neither DEM nor NDVI evidence suggests that significant overland flow or associated sediment from Thurgood Canyon made it all the way to Salt Creek between 2013 and 2021. During this period, the maximum observed flow was 32 m^3/s, and the maximum modeled flow was 96 m^3/s. Based on these findings, it is highly unlikely more frequent flood events will deliver overland flow and associated sediment directly to Salt Creek with the current drainage infrastructure and no diversion of flow south of the main channel. Despite this, it is possible that large, infrequent events, such as a 100 yr or larger event, could deliver overland flow all the way to Salt Creek. It is also likely that such an event could damage culvert 1 given the significant scour caused by numerous smaller events.

Figure 40. HEC-HMS hydrographs for 2013–2018 and 2020.

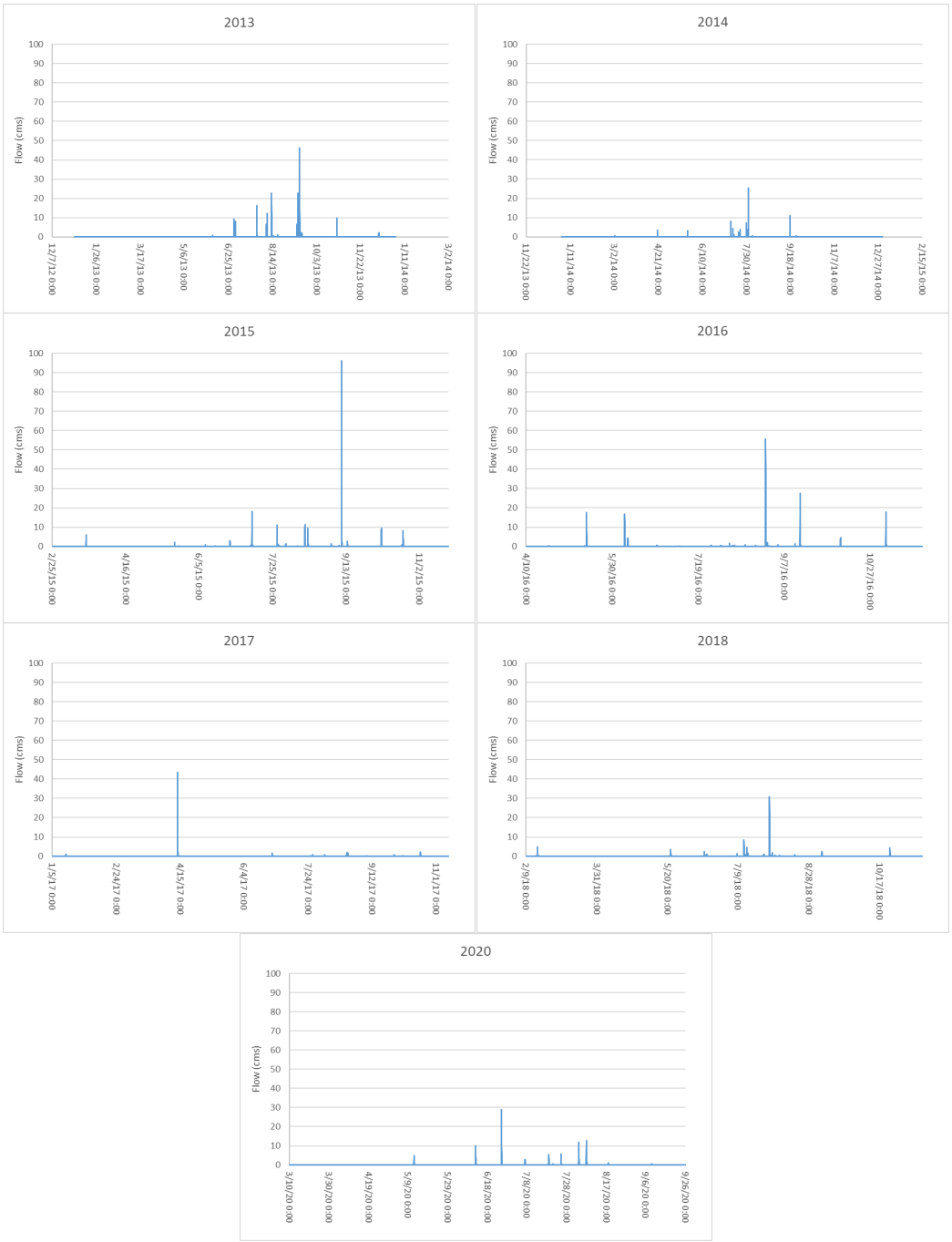

3.5 Hydraulics

The HEC-RAS model was forced using the proposed maximum peak flow events as determined by USACE Tulsa District (Table 3). Three versions of the model were created based on the three available DEM data sets. Specifically, the south berm was adjusted in the model to accurately reflect its form and structure as determined from the three DEMs. The scour holes were broadened and deepened to reflect scour processes or made narrower or shallower to reflect any maintenance or deposition occurring between 2013 and 2019 or between 2019 and 2021.

In 2013, the berm was mostly intact, with only scour hole 4 allowing flow to leave the main channel, an average of 3% of peak flow (Table 17). By 2019, scour hole 4 had partially aggraded due to local deposition, but scour hole 2 had become deeper and wider, allowing 7%–18% of peak flow to leave the main channel. By spring of 2021, scour holes 1 and 3 had also become broader and deeper. Scour hole 1 had not yet broken completely through the berm, while flow escaped through scour hole 3 only during events larger than the 2 yr event. In 2021, scour holes 2 and 4 together allowed 5%–17% of peak flow to leave the main channel during flow events ranging from the 1 to 100 yr events.

Table 17. Percentage of total flow at Culvert 1 or diverted through the scour locations for different design floods under four scenarios.

		1 yr	2 yr	5 yr	10 yr	25 yr	50 yr	100 yr
Main Culvert	2013	97%	97%	97%	97%	97%	98%	98%
	2019	93%	91%	89%	87%	85%	83%	82%
	2021	95%	91%	88%	86%	84%	82%	81%
	Proposed	62%	63%	65%	65%	66%	66%	66%
		1 yr	**2 yr**	**5 yr**	**10 yr**	**25 yr**	**50 yr**	**100 yr**
Scour hole 1	2013	0%	0%	0%	0%	0%	0%	0%
	2019	0%	0%	0%	0%	0%	0%	0%
	2021	0%	0%	0%	0%	0%	0%	0%
	Proposed	20%	20%	19%	19%	18%	18%	18%
		1 yr	**2 yr**	**5 yr**	**10 yr**	**25 yr**	**50 yr**	**100 yr**
Scour hole 2	2013	0%	0%	0%	0%	0%	0%	0%
	2019	7%	9%	11%	13%	15%	17%	18%
	2021	3%	6%	8%	9%	11%	12%	13%
	Proposed	7%	8%	8%	8%	8%	8%	8%
		1 yr	**2 yr**	**5 yr**	**10 yr**	**25 yr**	**50 yr**	**100 yr**
Scour hole 3	2013	0%	0%	0%	0%	0%	0%	0%
	2019	0%	0%	0%	0%	0%	0%	0%
	2021	0%	0%	1%	1%	2%	2%	3%
	Proposed	0%	0%	0%	0%	0%	1%	1%
		1 yr	**2 yr**	**5 yr**	**10 yr**	**25 yr**	**50 yr**	**100 yr**
Scour hole 4	2013	3%	3%	3%	3%	3%	2%	2%
	2019	0%	0%	0%	0%	0%	0%	0%
	2021	2%	3%	3%	4%	4%	4%	4%
	Proposed	11%	9%	9%	8%	8%	7%	7%

As noted in Section 3.3.3, evidence suggests that only culvert 2 experienced flow originating from spillover directly from the main drainage channel, most of which originated from scour hole 4. Historic drainage patterns suggest that flow from scour hole 2 could eventually drain through culverts 3 or 5, but no evidence suggests any overland flow made it from scour hole 2 to RR7 at any location between 2013 and 2019.

All flow from scour holes 3 and 4 was assumed to pass through culvert 2. Half of the flow from scour hole 2 was assumed to pass through culverts 3 and 5. Under all scenarios, culverts 1, 4, and 5 were not overtopped for any event. Culverts 2 and 3 were never overtopped during the 2013 scenario when limited flow escaped from sour hole 4. However, both culverts were overtopped for all events greater than the 2 yr event under the 2019 and 2021 scenarios when scour hole 4 was larger.

These findings indicate that culverts 2–5 are sized correctly to provide local drainage for the southern portions of the fan (drain runoff resulting from rainfall directly on the fan). Culverts 2 and 3 are too small to accommodate any moderate to significant overland flow leaking from the main Thurgood drainage channel via scour holes 2, 3, or 4.

Given the historic channels to the south of the main channel and the history of scour along the main channel berm, much of the overland flow in Thurgood Canyon would spread to the south and east if no control structures (berms) existed on the alluvial fan. The existing primary berm forces the majority of flow to pass under RR7 at one location, increasing the energy and sediment load capacity of the flow further down the fan than would otherwise be the case. If a greater portion of flow was diverted to the south before reaching RR7, the likelihood of damage to RR7 or of direct impacts to Salt Creek would be lowered.

A proposed scenario was modeled to investigate the feasibility of controlled flow diversions to the south. The four scour locations were modeled as controlled weir flow diversion locations, assuming gabion baskets and mattresses were used to create reinforced weir structures. Under this scenario, secondary berms or grading would be used to divert flow from scour location 1 along the base of the mountain range and flow from scour location 2 to the culvert 5 subwatershed (Figure 41). The weir at scour location 1 would be sized to divert approximately 20% of the peak flow from the main channel across all modeled flow events. Weirs at scour locations 2 and 4 would be sized to divert approximately 8% of peak flow each (Figure 42 and Figure 43). Total flow in the main channel at RR7 would be reduced to two-thirds of the peak flow from Thurgood Canyon (Table 17). The reduced flow in the main channel also lowers the average exit velocity from culvert 1 by 10%, which would reduce scour just downstream of RR7 and reduce the likelihood of structural failure.

Under existing conditions, culvert 2 is too small to pass flow currently diverted from the main channel for all flow events larger than the 2 yr event. As scour holes 3 and 4 become larger, the magnitude and occurrence of flow through culvert 2 will increase, increasing the likelihood of overtopping and structural failure. Under the proposed scenario the magnitude and occurrence of flow through culvert 2 would increase. To accommodate existing and possible future flow events, culvert 2 should be replaced with a twin 2.44 × 2.44 m box culvert, matching culvert 5.

Figure 41. Thurgood Canyon alluvial fan detailing locations of existing berm scour locations and culverts and proposed secondary berms, drainage channels, and drainage divides to the south of the main drainage channel.

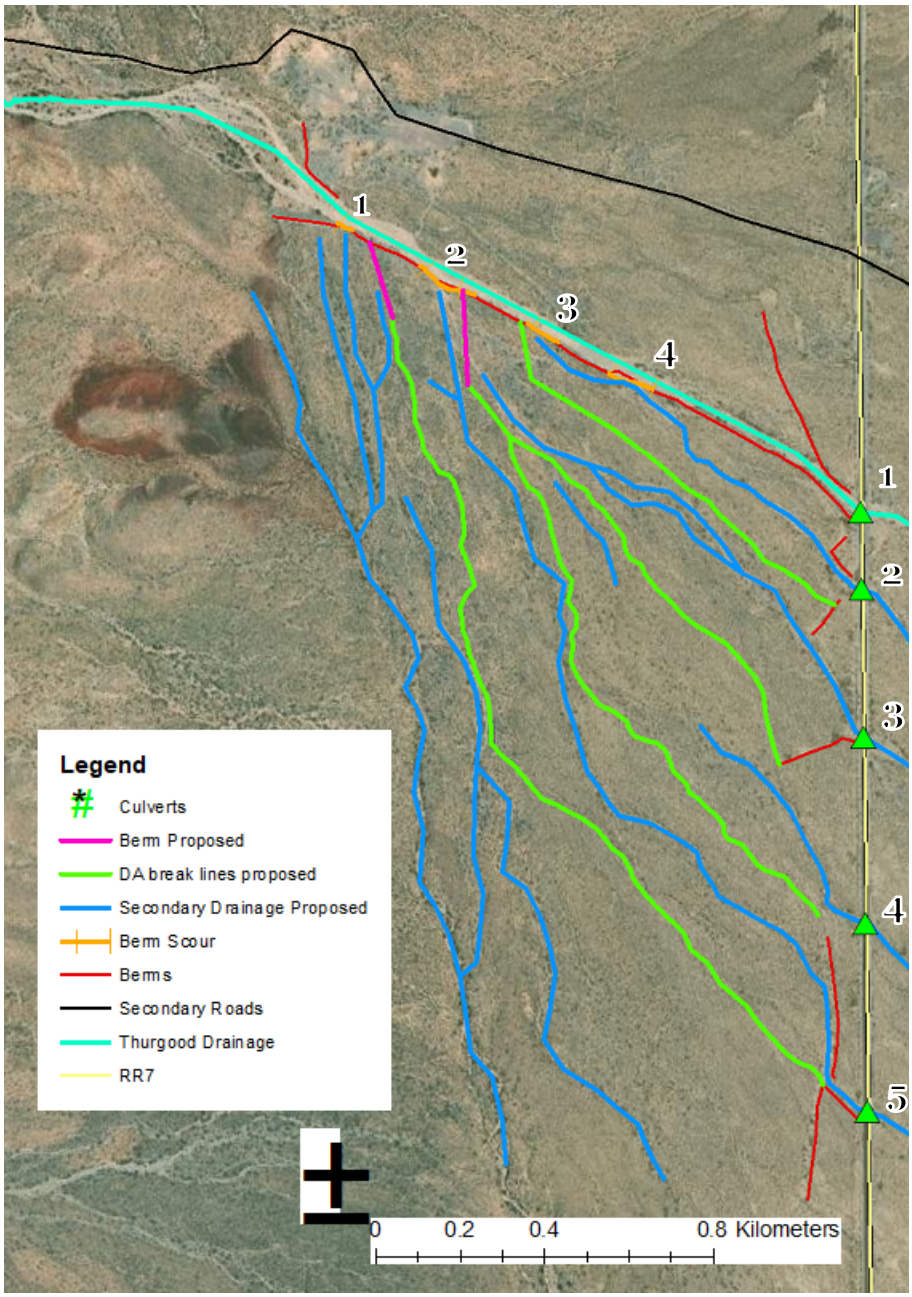

Figure 42. Scour hole shape and size progression from 2013 to 2021, including dimensions of proposed constructed diversion weirs, at scour locations 1 and 2.

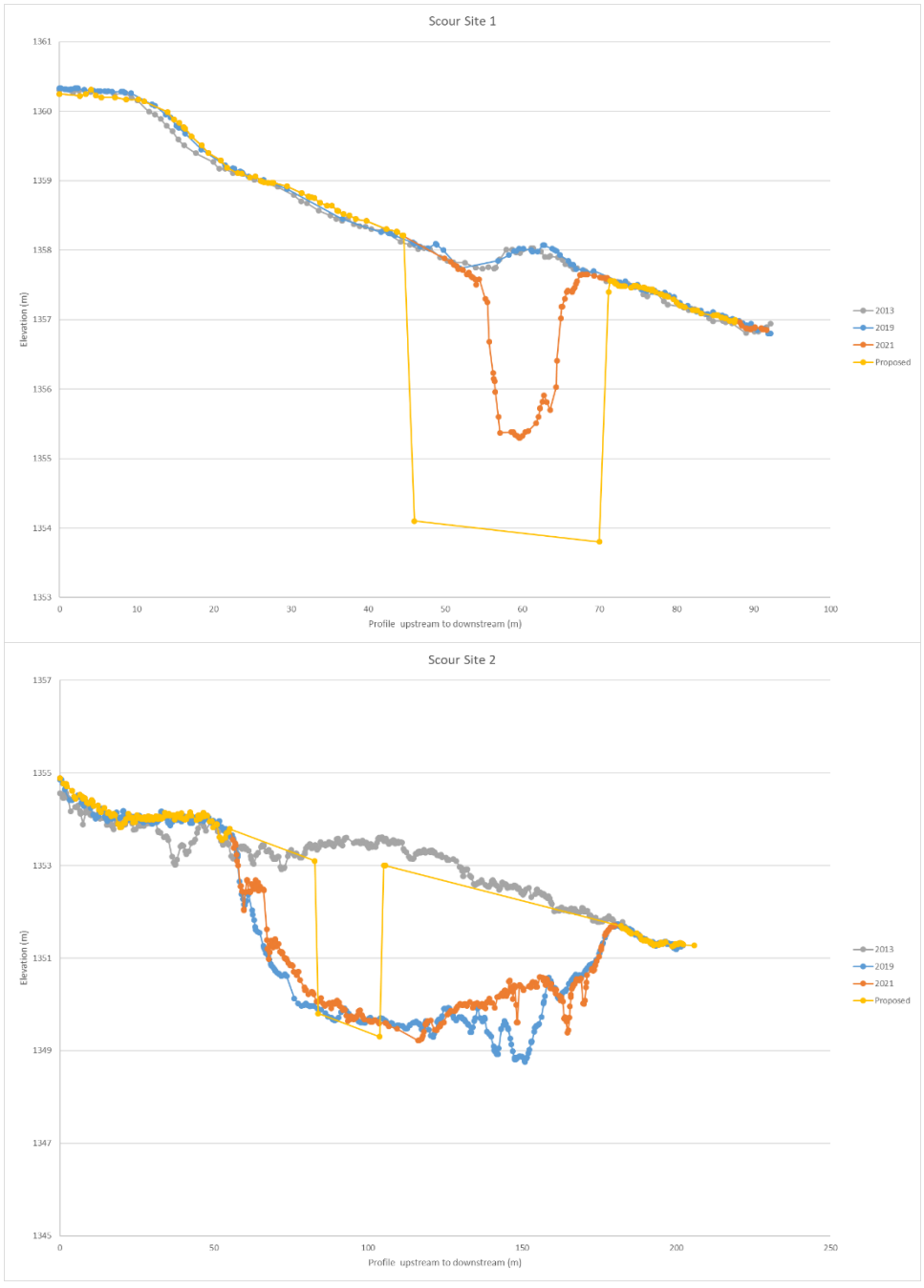

Figure 43. Scour hole shape and size progression from 2013 to 2021, including dimensions of proposed constructed diversion weirs, at scour locations 3 and 4.

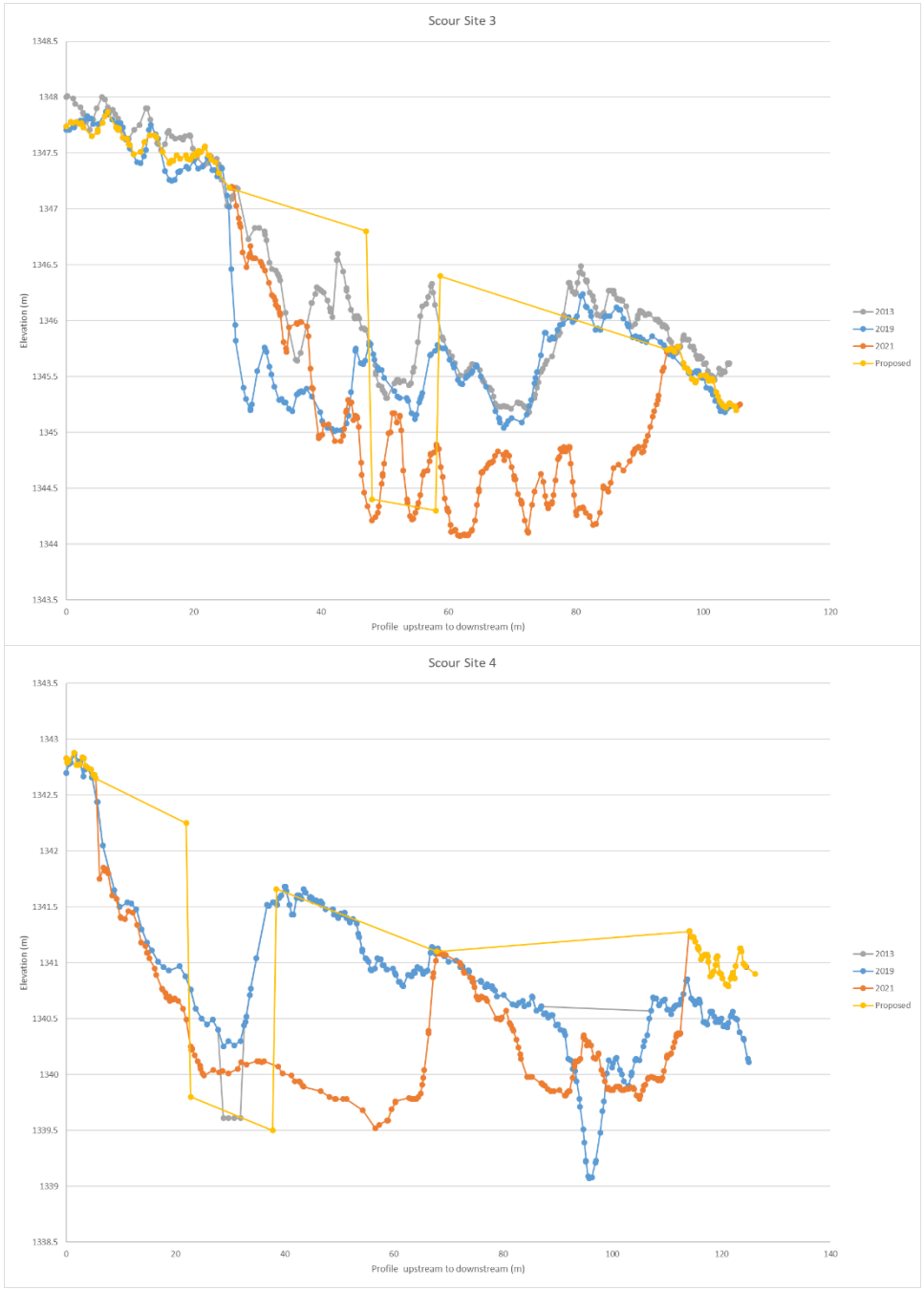

4 Conclusions

The following conclusions are based on the comprehensive assessment presented above:

Potential impacts to Salt Creek

- Frequent to moderately rare (small to medium) flood events do not transport overland flow and sediment to Salt Creek. Most overland flow spreads out into numerous preferential flow channels past RR7 and infiltrates before reaching Salt Creek.
- Only very rare (very large) flood events could potentially transport overland flow and sediment directly to Salt Creek.
- The current drainage infrastructure maintains a single, large channel from the fan apex to just downstream of RR7, which maintains the flow energy and sediment carrying capacity further down the fan than would occur absent the drainage infrastructure. However, the flow energy begins to dissipate within 500 m downstream of RR7, preventing direct impacts to Salt Creek except possibly in the case of very rare events. New channel scour could not be detected more than 3,000 m downstream of RR7 since 2011.
- Returning flow to historic flow patterns will increase opportunity for infiltration thus recharging the groundwater aquifer. This will provide more consistent groundwater flow to Salt Creek, improving habitat for the White Sands pupfish.

Sediment load

- The total annual sediment load delivered onto the Thurgood alluvial fan is estimated at thousands of metric tons per year but varies significantly depending on the number and magnitude of events. The suspended sediment load, mostly sand, comprises the majority of the total sediment load, while larger but less numerous particles make up the bedload. Based on the GIS assessment and site visits, the majority of the sediment load is deposited within 1,000 m downstream of RR7.

Current drainage infrastructure

- The current drainage infrastructure is designed to channelize drainage from Thurgood Canyon through one large culvert under RR7. This design limits the number of locations at which RR7 can be flooded or damaged.
- The flow energy and volume has caused significant scour downstream of culvert 1 where a portion of the gabion mattress is beginning to fail.
- The primary berm on the south side of the main drainage channel is prone to scour at four locations. The wire-mesh-reinforced portion of the berm just upstream of RR7 shows no signs of scour or failure. Also, the gabion baskets located on the culvert 1 abutments show no signs of failure.
- A portion of flow from the main channel is diverted through scour location 4 to culvert 2 under existing conditions. Culvert 2 is undersized to allow passage of flow originating from the main channel.
- A portion of flow from the main channel is also diverted through scour location 2, but no overland flow from this location seems to reach RR7 at this time.
- CMP culverts are not suitable on the Thurgood alluvial fan due to the significant sediment loads and vulnerability to clogging.

5 Recommendations

5.1 Overview

The flow events from Thurgood Canyon are high energy and carry significant sediment loads and large individual particle sizes. Sediment control BMPs, such as sedimentation basins or in-channel flow control structures like bendway weirs or rock vanes are not feasible on this alluvial fan. Maintaining a single channel past RR7 minimizes the number of locations at which significant overland flow crosses under the roadway but increases the risk of culvert failure at RR7 and the likelihood of negative impacts downstream. As a result, we recommend controlled flow diversions to the south, upstream of RR7, accomplished by static gabion weirs (or comparable structures). Controlled diversions will decrease negative impacts downstream and the likelihood of culvert 1 failing. In addition, these diversions utilize a portion of the alluvial fan not currently used for military testing or training.

Controlled flow diversion at scour location 1 would send flow to the south for more than 3 km before potentially crossing RR7. Given the GIS analysis of overland flow downstream of RR7, it is highly likely all flow diverted at scour location 1 would infiltrate before reaching RR7 south of culvert 5. Flow diversion at this location at 20%–25% of peak flow is recommended.

Flow diverted at scour location 2 will flow to culvert 5 if minor grading and secondary berming is completed. Culvert 5 is already sized appropriately, and given the distance traveled, only rare flow events would reach culvert 5. Flow diversion at this location at 8%–10% of peak flow is recommended.

Flow diverted at scour location 4 will flow to culvert 2, as it does under current conditions. However, culvert 2 is undersized and should be enlarged if a third flow diversion weir is constructed. Alternatively, this section of the primary berm can be reconstructed and reinforced with wire mesh or Reno Mattress BMPs. If a third weir is installed, diversion of 8%–10% of peak flow is recommended at this location.

Scour location 3 and all other berm sections prone to scour should be reinforced with wire mesh riprap or Reno Mattress BMPs. All flow diversion weirs should be constructed from gabion baskets or concrete and pro-

tected from scour. Abutments should be protected from scour using gabion baskets. On the downstream side, abutments should be given additional protection using gabion mattresses, impact basins, or other BMPs designed with best engineering judgement following a scour analysis.

Given the sediment loads expected at any location on the alluvial fan, box culverts are generally preferable to CMP culverts because they are less likely to be clogged with sediment and are more likely to be self-cleaning.

The following is an operations and maintenance plan for the Thurgood alluvial fan prioritized by action item and long-term planning.

5.2 Long-term O&M

All drainage infrastructure on the Thurgood alluvial fan shall be inspected once a year in November at the end of the wet season. All flow control berms shall be inspected along their length, and scour locations documented. All active scour locations shall be measured and compared to the previous years' measurements. Culvert inspections should note overall condition, evidence that the roadway has been overtopped or any high-water marks, scour upstream or downstream, and if the culvert contains any debris. Culverts 1–5 shall be inspected. Flow diversion structure inspections should note overall condition, any high-water marks, and scour upstream or downstream.

Required maintenance, as determined by the annual inspection, shall be completed before mid-May, the beginning of the following wet season.

When new lidar data become available with coverage over the Thurgood alluvial fan, an updated assessment shall be completed. The assessment shall focus on potential Salt Creek impacts, drainage infrastructure integrity, and potential impacts of flow diversions to the south of the main channel.

New BMPs, culverts, and diversion weirs shall be designed using best engineering judgment and installed consistent to relevant New Mexico Department of Transportation specifications. Scour analysis shall be included as part of the engineered design for all culverts and diversion weirs. Minimum scour BMPs shall include gabion baskets, concrete impact structures, gabion/Reno Mattresses, and wire-mesh-reinforced riprap as appropriate.

Alternative scour BMPs may be used only with written approval from either WSMR ITAM or WSMR Department of Public Works (DPW) as appropriate.

5.3 Action items

High Priority

1. Monitor gabions and Reno Mattress downstream of culvert 1 and stabilize/repair as required.
2. Repair primary berm at scour location 4 to prevent damage to the existing culvert 2 and damage to RR7.
3. Reinforce primary berm at scour location 3 with wire mesh BMP.
4. Implement a flow diversion strategy beginning with
    a. A diversion weir and required secondary flow path controls at scour location 1, the highest-priority diversion location
    b. A diversion weir and required secondary flow path controls at scour location 2. If flow diversion weir is not installed at this location the primary berm shall be rebuilt and reinforced with wire mesh riprap or Reno Mattress to prevent scour.
    c. A diversion weir and required secondary flow path controls at scour location 4. Replace culvert 2 with a dual 2.44 × 2.44 m box culvert, including downstream scour BMP. If a flow diversion weir is not installed at this location, the primary berm shall be rebuilt and reinforced with wire mesh riprap or Reno Mattress to prevent scour.

Lower Priority

1. Replace culvert 3 with a single 2.44 × 2.44 m box culvert, including downstream scour BMP.
2. Replace culvert 4 with a dual 2.44 × 2.44 m box culvert, including downstream scour BMP.

References

Ahbari, A., L. Stour, A. Agoumi, and N. Serhir. 2018. "Estimation of Initial Values of the HMS Model Parameters: Application to the Basin of Bin El Ouidane (Azilal, Morocco). *J Mater Environ Sci* 9(1), 305–317.

Bennett, Todd Howard. 1998. "Development and Application of a Continuous Soil Moisture Accounting Algorithm for the Hydrologic Engineering Center Hydrologic Modeling System (HEC-HUMS)." PhD diss, University of California, Davis.

Bennett, Todd H., and John C. Peters. 2000. "Continuous Soil Moisture Accounting in the Hydrologic Engineering Center Hydrologic Modeling System (HEC-HMS)." In *Building Partnerships: Proceedings of the 2000 Joint Conference on Water Resources Engineering and Water Resources Planning and Management*, Minneapolis, MN, 30 July–2 August 2000, edited by Rollin H. Hotchkiss and Michael Glade, 1–10. Reston, VA: American Society of Civil Engineers.

Blair, Terence C., and John G. McPherson. 1994. "Alluvial Fans and Their Natural Distinction from Rivers Based on Morphology, Hydraulic Processes, Sedimentary Processes, and Facies Assemblages." *Journal of Sedimentary Petrology* 64 (3)*:* 450–489.

Church, M., J.F. Wolcott, and W.K. Fletcher. 1991. "A Test of Equal Mobility in Fluvial Sediment Transport: Behavior of the Sand Fraction." *Water Resources Research* 27 (11): 2941–2951.

Department of the Army. 2007. *Environmental Quality, Environmental Protection and Enhancement*. Army Regulation 200-1. Washington, DC: Department of the Army. https://armypubs.army.mil/epubs/DR_pubs/DR_a/pdf/web/r200_1.pdf.

Gomez-Villar A. and J.M. Garcia-Ruiz. 2000. "Surface Sediment Characteristics and Present Dynamics in Alluvial Fans of the Central Spanish Pyrenees." *Geomorphology* 32, nos. 3–4 (September): 127-144. https://doi.org/10.1016/S0169-555X(99)00116-6.

Harter, Thomas, and Jan W. Hopmans. 2005. "Role of Vadose-Zone Flow Processes in Regional-Scale Hydrology: Review, Opportunities and Challenges." In *Unsaturated-zone Modeling: Progress, Challenges and Applications*, edited by R.A. Feddes, G.H.de Rooij, and J.C. van Dam, 179–208. Vol. 6 of *Frontis*. Wageningen, Netherlands: Wageningen University and Research.

Holberg, Jessica. 2014. "Tutorial on Using HEC-Geohms to Develop Soil Moisture Accounting Method Inputs for HEC-HMS." Purdue University, West Lafayette, IN. https://web.ics.purdue.edu/~vmerwade/education/hechms_sma.pdf.

Lin, Y. 2011. GCIP/EOP Surface: Precipitation NCEP/EMC 4km Gridded Data (GRIB) Stage IV Data, Version 1.0. UCAR/NCAR Earth Observing Laboratory; accessed 17 August 2018. https://doi.org/10.5065/D6PG1QDD.

Linsley Jr., Ray K., Max Adam Kohler, and Joseph L. H. Paulhus. 1975. *Hydrology for Engineers*. New York: McGraw-Hill.

MacArthur, Robert C., M. D. Harvey, and E. Sing. 1990. *Estimating Sediment Delivery and Yield on Alluvial Fans*. TP-130. Davis, CA: US Army Corps of Engineers, Hydrologic Engineering Center. https://www.hec.usace.army.mil/publications/TechnicalPapers/TP-130.pdf.

McMahon, Patrick Lasater. 2013. "Bedload Transport Sampling, Characterization and Modeling on a Southern Appalachian Ridge and Valley Stream." PhD diss., University of Tennessee.

Mockus, V., 1961: Watershed Lag. Doc. ES-1015, US Department of Agriculture, Soil Conservation Service, Washington, DC.

Muñoz Sabater, J. 2019. ERA5-Land Hourly Data from 1981 to Present. Copernicus Climate Change Service (C3S) Climate Data Store (CDS); accessed on 15 November 2021. https://doi.org/10.24381/cds.e2161bac.

NPS (National Park Service). 2022. *NPS Boundary*. Shapefile. Last Modified 13 April 2022. https://public-nps.opendata.arcgis.com/datasets/nps::nps-boundary-1/explore?location=7.032407%2C-12.497900%2C2.63

Naus, C. A., R. G. Myers, D. K. Saleh, and N. C. Myers. 2014. *Compilation of Hydrologic Data for White Sands Pupfish Habitat and Nonhabitat Areas, Northern Tularosa Basin, White Sands Missile Range and Holloman Air Force Base, New Mexico, 1911–2008*. No. 810. Albuquerque, NM: US Geological Survey. https://pubs.usgs.gov/ds/810/.

Noirni, Gianluca, Maria C. Zuluaga, Iris J. Ortiz, Dakila T. Aquino, Alfredo Mahar F. Lagmay. 2016. "Delimitation of Alluvial Fans from Digital Elevation Models with a GIS Algorithm for the Geomorphological Mapping of the Earth and Mars." *Geomorphology* 273: 134–149. https://doi.org/10.1016/j.geomorph.2016.08.010.

NRCS (Natural Resources Conservation Service). 1997. "Irrigation System Design." *National Engineering Handbook: Part 652 Irrigation Guide*. Washington, DC: US Department of Agriculture. https://directives.sc.egov.usda.gov/OpenNonWebContent.aspx?content=17837.wba.

NRCS (Natural Resources Conservation Service). 2010. "Time of Concentration." *National Engineering Handbook*. Washington, DC: US Department of Agriculture. https://directives.sc.egov.usda.gov/OpenNonWebContent.aspx?content=27002.wba.

Pitlick, John, Yantao Cui, and Peter Wilcock. 2009. M*anual for Computing Bed Load Transport Using BAGS (Bedload Assessment for Gravel-bed Streams) Software*. RMRS-GTR-223. Fort Collins, CO: US Department of Agriculture, Forest Service, Rocky Mountain Research Station. https://doi.org/10.2737/RMRS-GTR-223.

Richards, G., and R. D. Moore. "Suspended Sediment Dynamics in a Steep, Glacier-Fed Mountain Stream, Place Creek, Canada." *Hydrological Processes* 17, no. 9 (2003): 1733–1753. https://doi.org/10.1002/hyp.1208.

Schaap, M. G., F. J. Leij, and M. T. van Genuchten. 2001. "ROSETTA: A Computer Program for Estimating Soil Hydraulic Parameters with Hierarchical Pedotransfer Functions." *J. Hydrol.* 251: 163–176, https://doi.org/10.1016/S0022-694(01)00466-8.

SSURGO (Soil Survey Geographic). 2019. Database for New Mexico, Natural Resources Conservation Service, United States Department of Agriculture; accessed 12 June 2019. https://websoilsurvey.nrcs.usda.gov/.

Sterling, Shannon M., and Michael Church. 2002. "Sediment Trapping Characteristics of a Pit Trap and the Helley-Smith Sampler in a Cobble Gravel Bed River." *Water Resources Research* 38, no. 8 (August): 19-1–19-11. https://doi.org/10.1029/2000WR000052.

USACE (US Army Corps of Engineers). 2000. *Hydrologic Modeling System HEC-HMS Technical Reference Manual*. Davis, CA: Hydrologic Engineering Center.

USACE (US Army Corps of Engineers). 2018. "White Sands Missile Range Thurgood Canyon Watershed and Flood Inundation Modeling Study." Tulsa, OK: US Army Corps of Engineers, Tulsa District.

Waltemeyer, Scott D. 2001. *Estimates of Mountain-Front Streamflow Available for Potential Recharge to the Tularosa Basin, New Mexico*. US Geological Survey Water-Resources Investigations Report 01-4013. Albuquerque, NM: US Department of the Interior, US Geological Survey.

Waltemeyer, Scott D. 2008. *Analysis of the Magnitude and Frequency of Peak Discharge and Maximum Observed Peak Discharge in New Mexico and Surrounding Areas*. Scientific Investigations Report 2008-5119. Reston, VA: US Department of the Interior, US Geological Survey. https://doi.org/10.3133/sir20085119.

Weier, John, and David Herring. 2000. "Measuring Vegetation (NDVI & EVI)." Earth Observatory. NASA. Last modified 30 August 2000. https://earthobservatory.nasa.gov/features/MeasuringVegetation.

Wilcock, Peter R., and Joanna C. Crowe. 2003. "Surface-Based Transport Model for Mixed-Size Sediment." *Journal of Hydraulic Engineering* 129, no. 2 (February): 120–128. https://doi.org/10.1061/(ASCE)0733-9429(2003)129:2(120).

Wilcock, Peter R., John Pitlick, and Yantao Cui. 2009. *Sediment Transport Primer: Estimating Bed-Material Transport in Gravel-Bed Rivers*. RMRS-GTR-226. Fort Collins, CO: US Department of Agriculture, Forest Service, Rocky Mountain Research Station. https://www.fs.fed.us/rm/pubs/rmrs_gtr226.pdf.

Appendix A: Lab Methods

A.1 Particle size analysis

A.1.1 ASTM D6913 Dry Sieve

ERDC-CERL used the standardized ASTM D6913 sieve analysis for all bedload and shovel samples (Figure A-1). Samples that contained 5% of the total sample or 50 grams or greater on sieve #200 mm were separated out, and hydrometer analysis was conducted on that portion to determine clay content.

Figure A-1. Sieve nest in sieve shaker.

A.1.2 ASTM D7928 Hydrometer

Hydrometer analyses were performed using ASTM D7928: *Standard Test Method for Particle-Size Distribution (Gradation) of Fine-Grained Soils*

Using the Sedimentation (Hydrometer) Analysis. If greater than 5% passed the number 200 sieve, hydrometer analysis was performed.

The ASTM D4318: *Liquid Limit, Plastic Limit, and Plasticity Index of Soils* method was used to determine Atterberg limits. Soil sample sizes passing the number 40 sieve were required to be approximately 500 grams and 20 grams for liquid limit and plastic limit, respectively.

A.1.3 Coble size

A coble size analysis was completed on material that did not pass the 2-inch sieve after dry sieve analysis was completed. This material was measured on all three axes to classify each coble by size. The average coble size for each location was recorded.

A cobble size analysis was also performed on the armored layer within sample boxes A–N. The selected area was photographed and then any material cobble sized or larger was labeled, measured on all three axes of the stone, and recorded.

A.2 Total suspended sediments

ISCO samples were analyzed using ASTM D5907-09. All water samples were refrigerated upon receipt. Each bottled sample was treated as a single sample due to size. Total suspended soils were calculated by taking the weight of the dried sample divided by sample volume. Figure A-2 shows the product of the completed test of suspended sediment.

Figure A-2. Suspended sediment on filter paper.

Appendix B: HEC-HMS

The necessary initial parameters for the Soil Moisture Accounting method were estimated following Ahbari et al. (2018), Bennett and Peters (2000), and Holberg (2014) (Figure B-1). Saturated water content (field capacity), residual water content (wilting point), saturated hydraulic conductivity, and unsaturated hydraulic conductivity grids were generated using the NRCS Soil Survey Geographic database (SSURGO 2019) and the US Department of Agriculture (USDA) Agricultural Research Service (ARS) ROSETTA hydraulic parameter model (Schaap et al. 2001). Sand, silt, and clay percentage; bulk density at 15 bars; and water content percentage at 15 and 33 bars were extracted from the SSURGO database and imported into ROSETTA, with saturated water content, residual water content, saturated hydraulic conductivity, and unsaturated hydraulic conductivity as ROSETTA output. Soil storage and tension storage were estimated as the product of porosity and soil depth and the product of field capacity and soil depth, respectively. Soil depth was estimated as the lesser of root zone depth or soil restrictive layer depth, where root zone depth was estimated from land cover type (NRCS 1997), and soil restrictive layer depth was determined from the SSURGO database. Groundwater 1 (GW1) and 2 (GW2) percolation values were determined during calibration, but initial values were set at 50% and 10% of unsaturated hydraulic conductivity, respectively.

Figure B-1. Conceptual schematic of the continuous Soil Moisture Accounting method (USACE 2000).

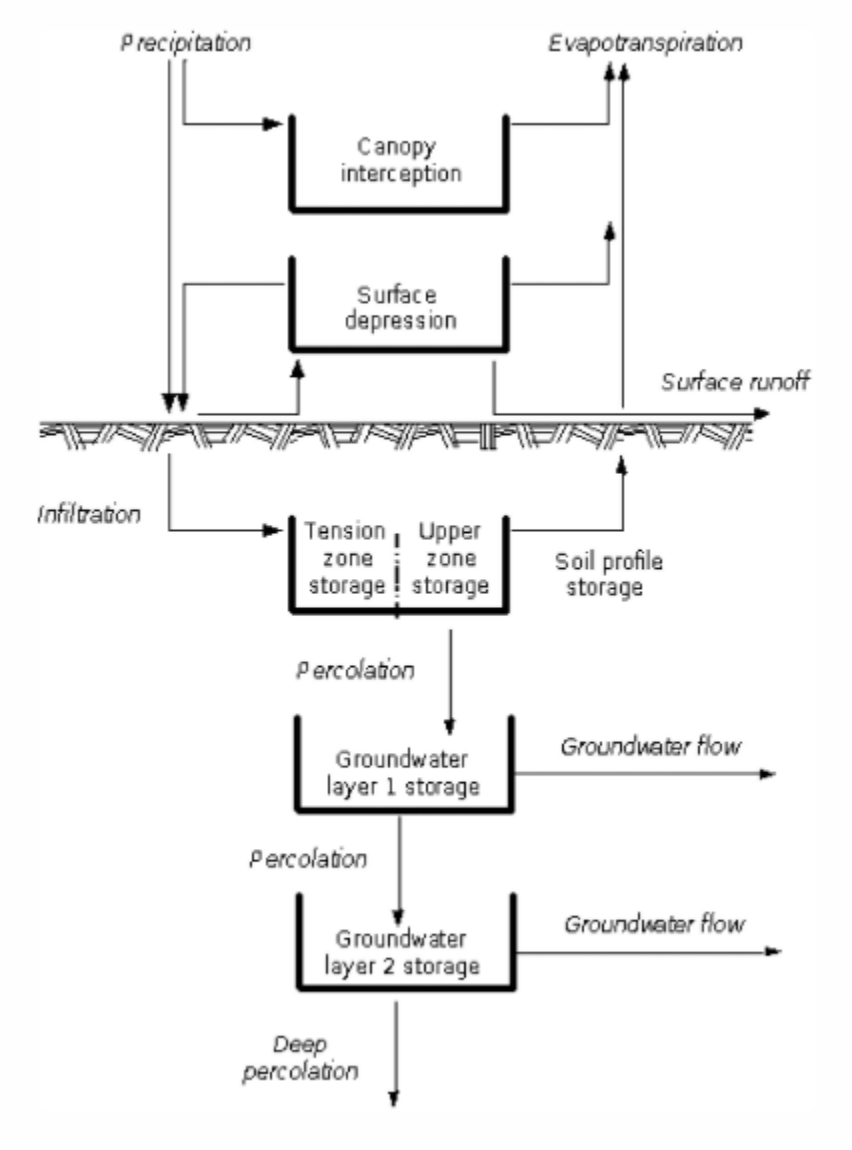

The four additional groundwater parameters, GW1 storage, GW1 coefficient, GW2 storage, and GW2 coefficient were estimated graphically by flow recession analysis developed by Linsley (1958). Hydrographs were plotted using the HOBO gage data for several isolated flow events to determine the separation of runoff, interflow, and baseflow (Harter et al. 2005). GW 1 parameters represent interflow, and GW 2 parameters represent baseflow (groundwater).

Surface depression storage was based on surface slope calculated from the National Elevation Dataset (NED) DEM and recommendations from Bennett (1998) (Table B-1). Canopy storage was calculated from National Land Cover Database (NLCD) land cover data and recommendations from (USACE 2000) (Table B-2).

Table B-1. Surface depression storage parameter values based on surface slope (Bennett 1998).

Description	Slope (%)	Surface Storage (mm)
Paved Impervious Areas	NA	3.18–6.35
Flat, Furrowed Land	0–5	50.8
Moderate to Gentle Slope	5–30	6.35–12.70
Steep, Smooth Slopes	>30	1.02

Table B-2. Vegetation canopy storage parameter values based on land cover type (USACE 2000).

Land Cover	Canopy Storage (mm)
Open Water	0
Developed	0
Barren	0
Deciduous Forest	2
Evergreen Forest	2.5
Mixed Forest	2.2
Shrub/Scrub	1.27
Herbaceous	1.27
Pasture/Hay	1.27
Cultivated Crops	1.27
Woody Wetlands	2.2
Herbaceous Wetlands	1.27

HEC-HMS requires the ModClark transform method be used with a gridded loss method. The ModClark method has two parameters, time of concentration and storage coefficient, that were estimated using the Soil Conservation Service (SCS) watershed lag method (Mockus 1961; NRCS 2010). The Muskingum–Cunge routing method was selected for its applicability in basins that are difficult to calibrate due to the lack of hydrograph observations. Routing parameterization was completed based on the 2019 DEM and data obtained during site visits.

HEC-HMS models are calibrated using gauge precipitation data or gridded precipitation data (e.g., radar data) in conjunction with stream gauge data

to validate modeled hydrographs with observed hydrographs for historic events. To calibrate and assess the continuous hydrologic models, they need to be forced with precipitation and evapotranspiration (ET) data that are as accurate as possible. Uncertainty in the precipitation and ET forcing would influence the comparison of streamflow observations and simulations, especially over long simulation timeframes. Therefore, the HEC-HMS models were forced with the National Centers for Environmental Prediction (NCEP) Stage IV (Lin 2011) quantitative precipitation estimation (QPE) and gridded ET estimates from ERA5-Land (Muñoz Sabater 2019). The Stage IV precipitation analysis is available on a 4 km grid across the continental United States (CONUS) and at 1 h temporal resolution. The ERA5-Land ET is available on a 0.1 × 0.1 degree grid across CONUS and at 1-h temporal resolution. HEC-HMS streamflow simulations, with Stage IV precipitation and ERA-Land ET forcing, were used to calibrate the models and then compared to HOBO observations to assess hydrologic model performance.

The initial soil water content (initial soil storage), initial GW1 storage, GW2 storage, canopy storage, and surface storage parameter values (as a percent of total depth) were determined using a warmup period on the HMS models. The Thurgood model was run for a 2 yr simulation, ending 31 December 2015, to determine storage parameter values for that date. The model was run again, starting the first of each month in 2015, with various initial storage values (%) to determine the optimum initial values and required warmup simulation length needed for the storage values to converge with the original long-term simulation. This analysis determined that soil storage required the most simulation time to converge but was only three months of model simulation time. A three-month warmup period was used for all calibration simulation runs.

HEC-HMS includes model optimization algorithms to calibrate models so that simulated results match observed streamflow as closely as possible. The optimization algorithms work by adjusting parameter values and initial conditions, including Manning's *n* for the routing method and the ModClark parameter values. Unfortunately, when the gridded SMA method is used, the optimization algorithms can only adjust the five storage initial conditions and the nongridded GW parameters, and none of the gridded parameter values (cover storage, surface storage, GW1 and GW2 storage, GW1 and GW2 coefficients, soil and tension storage, and saturated and unsaturated hydraulic conductivity).

To calibrate HEC-HMS models utilizing the gridded SMA method, a previously developed script was used to run the HEC-HMS models while changing one or more parameter values each run and saving the output. A range of gridded SMA parameter files were created for each parameter, ranging from 5% of the original estimated value(s) to 500%. Since tension storage must be smaller than soil storage, tension storage files with values ranging from 5% to 100% of the original estimated values and soil storage files with values ranging from 100% to 500% of the original estimated values were created. The HEC-HMS models were run while changing one parameter at a time for the full range of values to determine the model sensitivity to each parameter, and the outputs were compared to the available observed data both graphically and statistically. Many model parameters are physically based, and a wide range of possible values were outside of feasible parameter limits, but the entire range of parameter values were included to better assess model sensitivity to all parameters.

Abbreviations

ARS	Agricultural Research Service
BAGS	Bedload Assessment in Gravel-bed Streams
BMP	best management practices
CMP	corrugated metal pipe
DEM	digital elevation model
DPW	Department of Public Works
DS	downstream
CONUS	continental United States
ERDC-CERL	Engineer Research and Development Center, Construction Engineering Research Laboratory
ET	evapotranspiration
GIS	geographic information system
GW	groundwater
HEC-HMS	Hydrologic Engineering Center Hydrologic Modeling System
HEC-RAS	Hydrologic Engineering Center River Analysis System
IR	infrared
ITAM	Integrated Training Area Management Program
NAIP	National Agricultural Imagery Program
NCEP	National Centers for Environmental Prediction

NED	National Elevation Dataset
NDVI	normalized difference vegetation index
NLCD	National Land Cover Database
NIR	near-infrared radiation
QPE	quantitative precipitation estimation
RMSE	root-mean-square error
SCS	Soil Conservation Service
SMA	soil moisture accounting
TSS	total suspended solid
WSMR	White Sands Missile Range
WSNP	White Sands National Park
UAS	unmanned aerial system
USACE	US Army Corps of Engineers

REPORT DOCUMENTATION PAGE

Form Approved
OMB No. 0704-0188

1. REPORT DATE (DD-MM-YYYY)	2. REPORT TYPE	3. DATES COVERED (From - To)
09/01/2022	Final Report	

4. TITLE AND SUBTITLE
White Sands Missile Range Thurgood Canyon Watershed: Analysis of Range Road 7 for Development of Best Management Practices and Recommendations

5a. CONTRACT NUMBER

5b. GRANT NUMBER

5c. PROGRAM ELEMENT

6. AUTHOR(S)
Daniel R. Gambill, Matthew M. Stoklosa, Sean A. Matus, Heidi R. Howard, and Garrett R. Feezor

5d. PROJECT NUMBER

5e. TASK NUMBER

5f. WORK UNIT NUMBER

7. PERFORMING ORGANIZATION NAME(S) AND ADDRESS(ES)
US Army Engineer Research and Development Center (ERDC)
Construction Engineering Research Laboratory (CERL)
2902 Newmark Dr.
Champaign, IL 61824

8. PERFORMING ORGANIZATION REPORT NUMBER
ERDC/CERL TR-22-11

9. SPONSORING / MONITORING AGENCY NAME(S) AND ADDRESS(ES)
White Sands Missile Range, Integrated Training Area Management
Washington, DC 20314-1000

10. SPONSOR/MONITOR'S ACRONYM(S)

11. SPONSOR/MONITOR'S REPORT NUMBER(S)

12. DISTRIBUTION / AVAILABILITY STATEMENT
Distribution Statement A: Approved for public release; distribution is unlimited.

13. SUPPLEMENTARY NOTES
MIPR 11305306

14. ABSTRACT

Thurgood Canyon, located on White Sands Missile Range (WSMR), contains an alluvial fan that is bisected by a primary installation road and is in the proximity of sensitive fish habitats. This project was initiated to determine if and how sensitive fish habitats at the base of the fan are impacted by the existing drainage infrastructure and to assess the condition and sustainability of the existing transportation infrastructure. Findings show that the current drainage infrastructure maintains flow energy and sediment carrying capacity further down the fan than would occur in its absence. However, frequent to moderately rare (small to medium) flood events dissipate over 2 km from sensitive habitat, and overland flow and sediment do not reach the base of the fan. Controlled flow diversion is recommended upstream of the road to mitigate infrastructure or habitat impacts during very rare (very large) flood events. A comprehensive operation and management approach is presented to achieve sustainable transportation infrastructure and reduce the likelihood of impacts to the sensitive habitat.

15. SUBJECT TERMS
White Sands Missile Range (N.M.); Canyons; Alluvial fans; Drainage; Roads--Environmental aspects; Fishes--Habitat

16. SECURITY CLASSIFICATION OF:			17. LIMITATION OF ABSTRACT	18. NUMBER OF PAGES	19a. NAME OF RESPONSIBLE PERSON
a. REPORT	b. ABSTRACT	c. THIS PAGE			19b. TELEPHONE NUMBER (include area code)
Unclassified	Unclassified	Unclassified	SAR	93	